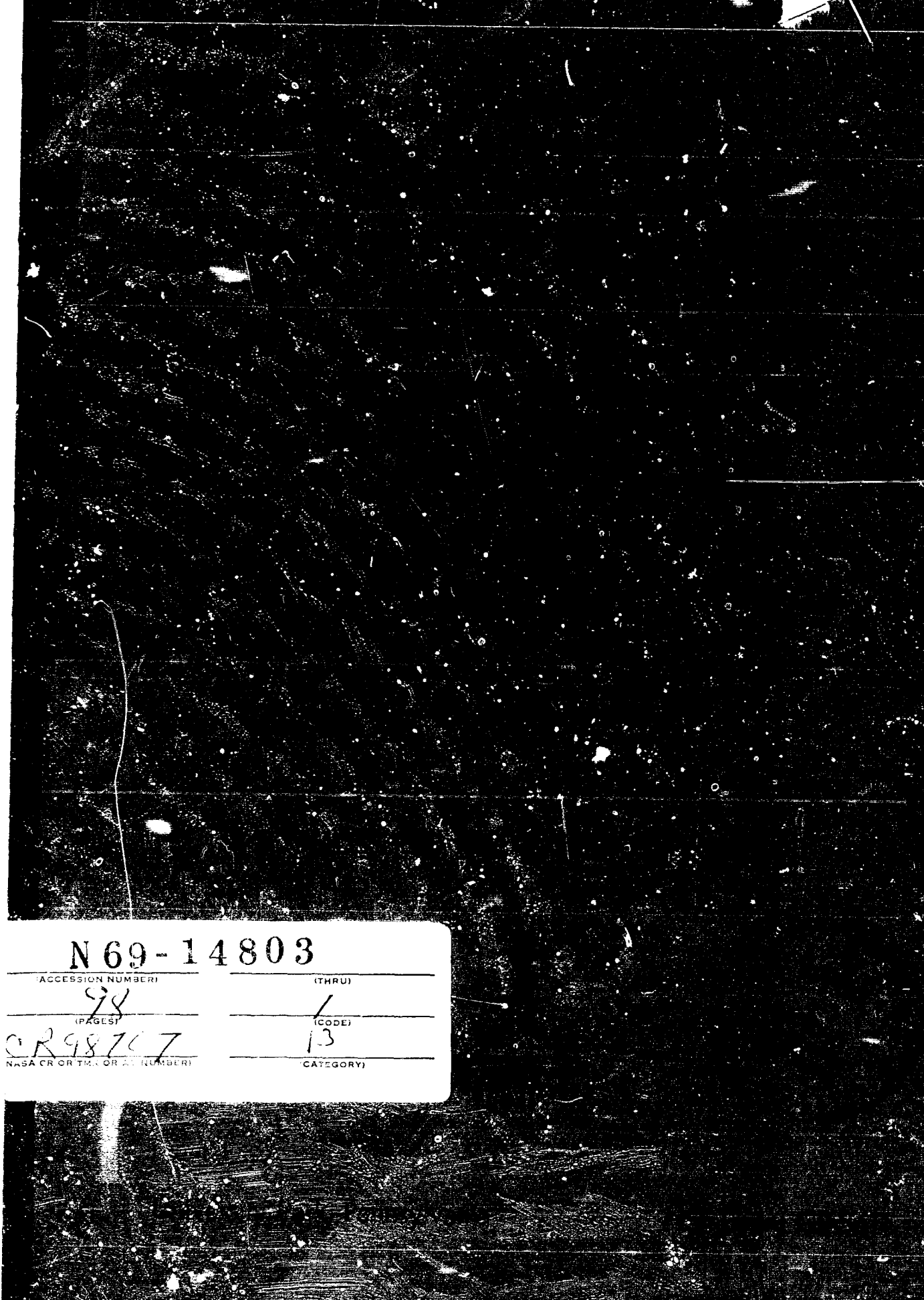

Ionospheric Research

NSF Grant GP-5611

Scientific Report

on

"Changes in the Upper Ionosphere During Severe Magnetic Storms"

by

D. G. Mack

September 30, 1968

Scientific Report No. 325

"The research reported in this document has been sponsored by the National Science Foundation under Grant GP-5611 and, in part, by the National Aeronautics and Space Administration under Grant NGR 39-009-095."

Ionosphere Research Laboratory

Approved for Distribution

A. H. Waynick, Director

The Pennsylvania State University

College of Engineering

Department of Electrical Engineering

ABSTRACT

Employing ionograms from the Alouette I topside sounder satellite, the moderately severe magnetic storms of June 15, 1965 and March 8, 1963 were investigated. Latitudinal contours of N(e) and vertical scale height revealed the disappearance of the geomagnetic anomaly during high magnetic activity, with a distinct correlation between Kp and the collapse of the anomaly being suggested. Storm-time variations of N(e) were found to be dependent upon the phase of the magnetic storm. Consistently reduced values of the storm-time vertical scale heights were interpreted as indicating an increased mean ionic mass due to an increased mixing of the ionosphere.

TABLE OF CONTENTS

CHAPTER I

INTRODUCTION AND GENERAL STATEMENT OF THE PROBLEM

Recognition of the fact that the ionosphere is greatly affected by geomagnetic storms has been long-standing. Historically, it has been well known from bottomside F-region studies of magnetic storm effects, employing foF2 data (notably, Appleton and Ingram, 1935; Berkner, Seaton, and Wells, 1939) and more recently, true height profile data (Thomas and Robbins, 1958; Somayajulu, 1963; Rishbeth, 1963), that subsequent to a magnetic storm, profound changes appear in the height and ionization density. Until recently however, the consequences of magnetic storms upon the upper ionosphere has been virtually unexamined due to the unavailability of sufficient topside data. With the launching of ionospheric satellites, such as the Alouette I and II, which have yielded valuable information on the topside ionosphere, and the refinement of computerized ionogram reduction techniques (Jackson, 1967; Doupnik and Schmerling, 1965; and Thomas et al.,1965), yielding a wealth of data, quickly yet accurately, on pertinent ionospheric parameters from topside ionograms, thorough studies of magnetic storm effects on the topside ionosphere have become feasible.

Morphological studies of the F-region disturbance conditions during geomagnetic storms were conducted by Appleton and Piggott (1952), Martyn (1953), Obayashi

(1952, 1954), Sinno (1953, 1954, 1955). Characteristic features deduced from these studies may be summarized as follows: Marked depression of the peak electron density, NmF2, possessing a pronounced diurnal variation, has been detected as high latitudes. However, in low latitudes, increases of NmF2 is most common, depressions being noted only during severe magnetic storms. In all cases the peak height hmF2 is found to increase. Fluctuations in middle latitudes display pronounced diurnal and seasonal control, exhibiting both depressions and enhancements of NmF2 depending upon the time of day and season.

Bottomside studies (Obayashi, 1964 and Matshushita, 1959) of magnetic storm effects on the ionosphere, inclusive of a wide range of latitudes, have revealed that, in general, ionospheric response to a magnetic storm consists of a raising of the peak height hmF2 at all latitudes, with corresponding peak electron density depressions at high and increases at low latitudes. In the mid-latitudes, depressions and enhancements of NmF2 may take place depending upon, as in the F-region studies, the local time and season.

Recently, information as collected from satellite measurements has yielded some valuable information on the response of the topside ionosphere to magnetic storms. Sayers (1964) reports considerable increases in the topside densities, N(e), for moderately disturbed conditions at high latitudes. Reddy, Brace, and Findlay (1967), from

an analysis of Tiros VII satellite data from 640 km, indicate strong intensifications of N(e) at middle and high latitudes on the dayside, with weaker intensifications on the nightside. Wilmore and Henderson (1965) report enhancements in the topside N(e) during periods of magnetic disturbances at high latitudes, with the gradual progression of these high latitude N(e) enhancements toward the near-equatorial latitudes as the storm intensifies. Most recently, both increases and decreases in the topside N(e) have been indicated by King et al. (1967), the particular response depending very heavily upon the respective latitude being affected. Somayajulu (1963) demonstrated that the Dst component of foF2 bears a remarkable resemblance to that of the geomagnetic field Dst component. Furthermore, Thomas and Venebles (1966) purport studies showing that the change in NmF2 at any mid-latitude station is determined by the geomagnetic storm main phase onset-time; concluding that when the onset-time takes place during night hours, it is accompanied by a decrease in NmF2 with either no change or an increase in NmF2 for onset-times occurring during the daytime.

Finally, Matsushita (1959, 1963) and Thomas and Robbins (1958) conducting an intensive statistical analysis of world-wide ionospheric data, confirmed the previously mentioned disturbed ionospheric characteristics and also demonstrated that the subpeak electron content fluctuates in a similar manner (Somayajulu, 1963). In addition, it has

been revealed from recent satellite measurements (Odishaw, 1964), that the total electron content of the topside ionosphere during a geomagnetic storm, behaves in the same manner, decreasing at middle and high latitudes while increasing at the near-equatorial latitudes.

Implications on the disturbed F-region theory precipitated by these results indicate real decreases and increases in the total electron content of the F-region under storm conditions, and not merely a redistribution (Somayajulu, 1963 and Titheridge and Andrews, 1967). Martyn (1953) suggests that vertical drift motions of the electrons, resulting from the interaction of the geomagnetic field with the magnetic storm generated electric field, identified with the geomagnetic Ds current system, contribute significantly to prominent diurnal variations in the disturbed F-region. In contrast, Matsuura (1963) and Yonezawa (1963) purport temperature changes induced by geomagnetic storms as being responsible for storm-time variations in the F-region. They demonstrated that N(e) production and loss rates and the diffusion rate would be affected by substantial increases in the F-region temperatures, thereby causing substantial N(e) variations.

However, the theory suggested by Matsuura and Yonezawa conflicts with results presented by Garriott and (1963) and Thomas (1966); indicating that under the proposed dependencies of production, loss, and diffusion upon temperature as presented by Garriott and Rishbeth (1963),

that the changes in Nm resulting from changes in the Te, Ti, and Tn (neutral gas temperature) are not sufficient to describe the large depletions detected during magnetic disturbances.

Thus, Martyn's interpretation of the geomagnetic Ds current system may possibly account for the ionospheric disturbance diurnal variations; however, the largest and most prominent variation of F2 storms, that of the storm-time variation Dst which may change by a factor of 4 to 10 during the storm main phase at the mid-latitudes, has of yet to be satisfactorily interpreted. This continues to be a prime consideration for future ionospheric storm theories in deriving a satisfactory and complete theory of ionospheric variations during magnetic storms.

From the preceding discussion, it is apparent that no completely satisfactory theory of ionospheric phenomena and its responsible causative mechanisms has yet appeared, although several promising theories have been proposed. Thus, the present study was undertaken in anticipation of deducing a more complete insight into the physical mechanisms responsible for the behavior of the topside ionosphere during severe magnetic storms. In this respect, the subsequent sections of this study contain a resume of previous work concerning ionospheric changes detected during magnetic storms in addition to the results of the present investigation. Because of the intimate causative relation identified between geomagnetic storms and

ionospheric storms (defined as any substantial deviation of ionospheric or geomagnetic parameters from the mean), a well founded interpretation of storm-time ionospheric changes is highly dependent upon an understanding of magnetic storm phenomena. Thus, the following sections will present the here-to-fore deduced knowledge of magnetic storms.

CHAPTER II

SUMMARY THEORY OF THE F REGION

2.1 Introduction and Background

It is intended within this summary to present a simplified, yet not misleading, theory of the F region of the ionosphere. This review will, following a brief historical introduction, discuss primarily the physical processes which control particle densities, temperatures, and physical fluctuations in the F1 and F2 layers. First order explanations of F region phenomena, as yet unestablished, will be suggested.

The existence of ionized regions within the atmosphere was first postulated in the mid-nineteenth century to describe small fluctuations of the geomagnetic field, notably by Gauss (1839) and Stewart (1878). This hypothesis was revived by Kennelly (1902) and Heaviside (1902) to treat Marconi's transmission of radio signals across the Atlantic over the curvature of the earth. Direct proof of the downward reflection of radio waves from the ionosphere was concluded by Appleton and Barnett (1925). Shortly thereafter, Chapman presented a theory of formation of ionized layers in an idealized atmosphere (1931); thus, the stratified nature of the ionosphere was recognized. Since then, there has been a great deal of progress in this field; and today, the fundamental points in the mechanism of formation of the ionosphere may be considered well

understood. However, there are a number of problems of minor importance that must be solved for a better understanding of the detailed mechanism of layer formation. These "discrepancies" will be considered following a discussion of those physical processes responsible for layer formation.

The F region, which is considered as that part of the ionosphere which lies above 150 km, contains two discernible physical features involving the vertical distribution of electrons. These are the F1 "ledge" (100 to 200 km) and the F2 "peak" (250 to 400 km). The F region is formed by radiation in the range 170-911A acting principally on atomic oxygen, whereby the main ionic constituent becomes O^+. From photoionization rates of Hinteregger and Watanabe (1962) and density calculations by Bauer and Jackson (1962), it has been concluded that the electron density peak is well above the electron production peak, resulting from a rising electron density above 200 km due to a recombination rate that decreases more rapidly with height than the photoionization rate. This is in view of an exponentially decreasing electron loss rate having a value of 1×10^{-4}/s at 300 km. More recent investigations (Nisbet and Quinn, 1963 and Quinn and Nisbet, 1965) concerning the loss rate at night yield a loss rate varying with both temperature and season within the limits of 0.2 and 2.0×10^{-4}/s at

300 km. Their results suggest a seasonal change of composition which might have an important bearing on the seasonal anomaly in the F region.

F 2 layer: This layer shows a worked correlation with the geomagnetic field, having irregular spatial and temporal variation; such an irregularity is the equatorial anomaly. The variation with solar activity is also very prominent. From Allen (1948), the peak electron density can be expressed in the following form,

$$N_m = 5.9 \times 10^5 \ (1 + .02R) \cos(x)$$

where R is the relative sunspot number and (x) is the solar zenith angle. The level of the peak is normally situated at 300 km by day and 350 km by night in middle latitudes and at greater altitudes for higher solar activity and/or near the equator.

Fl layer: This layer is not so irregular as the F2 layer and its variation with solar activity is less marked. It merges into the F2 layer during the night and at times during the day cannot be distinguished as a separate layer. It is more liable to appear as a separate layer in summer than in winter and nearer noon than sunrise or sunset. The duration of the time for which this layer is observable in a day becomes shorter as the solar activity increases. From Allen (1948), the peak electron density in the daytime is given as follows:

$$N_m = 2.4 \times 10^5 \ ((1 + .0124R) \cos x)^{1/2}$$

The height of the peak level is 180 km.

2.2 Physical Processes

The following sections introduce the electron continuity equation and current physical processes believed to be responsible for the formation of the F region. First, the photochemical processes, reactions involving the production or loss of ionization, will be considered and subsequently, the transport processes, involving the physical movement of ionospheric plasma.

The continuity equation for electron density describes the temporal variation of the electron density n(h,t), and is given as follows:

$$\frac{\partial n}{\partial t} = q - l(n) - \text{div } (nv) \qquad (2.1)$$

where q and l represent the rates of production and loss of ionization, respectively, and (nv), where v is the drift velocity as derived from the force equation of the ionospheric plasma whose terms represent various forces acting on the plasma particles, representing the combined transport processes. The production and loss processes will be considered firstly.

Photoionization: Solar ultraviolet radiation is considered the principal source of ionization of the F region, having

an effective wavelength band of 170 to 911 A. The limits imposed on the effective wavelengths are determined by the ionization limits of the major constituents, 911 A for atomic oxygen, and 170 A for sufficient absorption coefficients. The incident flux of photons upon the upper atmosphere is 5×10^{14} m^{-2} s^{-1} at sunspot minimum. Prominent emission lines are HeII 304A, HeI 584A, and O V 630A.

To determine q, the rate of production of ionization, a single ionizing radiation acting on a single gas in a horizontally stratified atmosphere is considered; yielding, for any altitude:

$$q(h) = I\, n_e\, \sigma n(h)$$

where I is the photon flux, σ is the absorption cross-section, and n_e is an efficiency factor (electrons produced per photon absorbed). For more precise calculations, an obliquity factor sec x (x = zenith distance), the curvature of the earth, varying attenuations of incident flux caused by individual constituents, and wavelength dependence of the flux I and σ and n_e, must be considered. But for most purposes, Chapman (1931) provides an adequate and useful approximation to the production function q as:

$$q(z,x) = q_o \exp\,(1 - z - e^{-z} \sec(x))$$

where z is the reduced height and q applies to the case of a single radiation absorbed by a single constituent with scale height H independent of height.

Loss Processes: In that the F region is a rarefield region of the ionosphere, only two body collisions need be considered, implying that atomic ions will have difficulty in recombining with electrons; whereas, molecular ions, due to momentum and energy requirements, incur no such difficulty, sustaining recombination through dissociation. Because of this, formation of molecular ions from atomic ions is highly important in the F region. Important ionic reactions follow (Rishbeth, 1967):

$$O + h\nu \rightarrow O^+ + e \qquad \begin{matrix} O^+ + O_2 \rightarrow O_2^+ + O & \text{(a1)} \\ O_2^+ + e \rightarrow O + O & \text{(a2)} \end{matrix}$$

$$O + h\nu \rightarrow O^+ + e \qquad \begin{matrix} O^+ + N_2 \rightarrow NO^+ + N & \text{(b1)} \\ NO^+ + e \rightarrow N + O & \text{(b2)} \end{matrix}$$

In that the removal of electrons and atomic ions of oxygen is affected by a composite process of reactions (a) and (b), the mode of the process of electron removal is somewhat different at higher and lower altitudes in the F region, because reaction (a1) or (b1) becomes the rate-determining stage of the composite process at higher levels while reaction (a2) or (b2) becomes so at lower levels owing to the rapid decrease in the number densities of N_2 and O_2 with altitude.

For sufficiently low heights (F1 region),

$$q \simeq \alpha N^2$$

where (α) is the recombination coefficient and the rate of electron removal becomes of the recombination type there. For sufficiently high altitudes (F2 region), N_2 and O_2 are sufficiently low so that atomic ions O^+ are much more plentiful than molecular ions NO^+ and O_2^+, and reactions (a1) and (b1) become the rate-determining stage of the composite processes and the rate of removal of electrons is given:

$$q \simeq \beta N$$

where β is the attachment coefficient at sufficiently high altitudes and the rate of removal becomes of the attachment type there.

The following relation holds at the boundary between the F1 and F2 regions (Yonezawa, 1966):

$$\frac{\beta}{\alpha}(N_2) + \frac{\beta}{\alpha}(O_2) = N(e) \qquad (c)$$

Thus, the mode of removal of electrons is of an ion-atom interchange and recombination type in the F1 and F2 regions, respectively. However, the height of the level where (c) is satisfied is very sensitive to the values of

the parameters contained and is variable according to the circumstances. That is, if N(e) increases (or decreases), related conditions being unchanged, the level will be shifted to lower (or higher) heights.

There remains the question of the F2 peak, though, in that above the transition level $N = q/\beta$, which increases indefinitely upwards. Thus, the peak of the F2 region has yet to be accounted for. This will be accomplished through a consideration of transport processes which follows.

Transport Processes: The velocity (v) of the transport term, divergence of flux (v) contained in the continuity equation (2.1), is derived from the force equations which represent various forces acting on the electrons and ions (Rishbeth, 1967). Beyond the photoequilibrium region, the neutral density decreases sufficiently for plasma diffusion to become of increasing importance. The F2 electron peak marks a transition between the photoequilibrium region below and the diffusion region above. This transition represents a delicate balance between the competing processes of electron production, recombination, and plasma diffusion. The plasma diffusion term in the continuity equation is given:

$$DpN = \frac{D_o e^z}{H^2} \left(\frac{d^2N}{dz^2} + \frac{3dN}{2dz} + \frac{N}{2}\right) \qquad (2.2)$$

where D = the ambipolar diffusion coefficient and p is a differential operator.

Thus, the F2 layer continuity equation becomes:

$$\frac{\partial N}{\partial t} = q - \beta N + DpN \qquad (2.3)$$

From an analysis of this continuity equation, it may be demonstrated that the interaction of the controlling physical processes of production, recombination, and plasma diffusion determines the vertical distribution of ionization and the formation of NmF2. The consequences of diffusion can be considered rather simply through two separate conditions: the daytime equilibrium condition and the nighttime stationary condition where $\partial N/\partial t = 0$ and $q = 0$ are the criteria, respectively.

The following assumptions are to be considered: the ionization is in equilibrium ($\partial N/\partial t = 0$), which is justified in that the rate of change of N(e) negligible in comparison to the remaining terms of the continuity equation (Rishbeth and Barron, 1960). The region possesses a neutral gas temperature (Tn) and an electron temperature (Te) which are independent of height, but has an ion temperature (Ti) which is a function of height.

There are two limiting boundary conditions to be considered in the steady state continuity equation: chemical equilibrium where $q = \beta N$ and diffusive equilibrium where $DpN = 0$. Whether or not chemical or diffusive

equilibrium dominates is decided by the magnitude of the appropriate time constants, that is, the chemical and diffusion time constants.

The chemical time constant is given:

$$t_C = N/q = N/l$$

The diffusion time constant is given:

$$t_D = H^2/D$$

where H is the scale height of the N(e) distribution and D is the diffusion coefficient and is inversely proportional to the collision frequency (ν). Under the assumption that q and l are decreasing functions of height (Bauer, 1965), it is determined that t_C will increase with height whereas t_D will decrease, so that at a particular height level t_C will equal t_D. Considering the principal ionizable constituent to be atomic oxygen O, the photoionization of N_2 being negligible due to the rapid dissociative recombination of N_2^+ ions, it can be demonstrated that the condition $t_C = t_D$ becomes satisfied at roughly 300 km which conforms with the F2 peak criterion as presented by Rishbeth and Barron (1960).

For the daytime equilibrium condition, the following relationships are found to prevail at the peak: NmF2 takes place near the level where the loss rate ß and the diffusion

rate $d = D/H^2$ are the same. Below the peak diffusion becomes negligible and N(e) is accurately represented by $N = q/\beta$. This photochemical expression for N(e) roughly holds true at the peak. However, the photochemical terms q and βH rapidly lose their dominance above the peak (levels greater than 1 scale height above NmF2) and the distribution of N(e) is controlled by diffusion and follows and an exponential distribution.

For the nighttime equilibrium condition, photo-ionization ceases and N(e) decays at all heights with the same effective decay coefficient β' which is comparable to the daytime decay coefficient found at a level coincident with that where the nighttime peak is situated. (Rishbeth, 1967 and Stubbe, 1967).

2.3 F Region Anomalies

The Seasonal Anomaly: The unexplainably large measured values of midday foF2 developing in local winter and prominent at all geographic locations, particularly near latitudes of 50°, is called the seasonal anomaly. It has been suggested that this anomaly is due to changes of atmospheric composition, particularly of the ratio of O to N_2 (Rishbeth and Setty, 1964). The loss coefficient β depends on the concentration of molecular gases, this being primarily responsible for the increased electron densities.

The Equatorial Anomaly: The trough in the N(e) distribution of the near-equatorial latitudes, which is prominent during

the local time hours of 1000 to 2200 (King et al., 1964) and situated about the magnetic equator, possessing crests of ionization situated at 15^{o} to 20^{o} latitude on both sides of the magnetic equator, constitutes an anomaly to the simple theory of formation of the ionosphere by production and loss, which predicts a single maximum for a direct overhead sun. The most favorable theory at present is Martyn's (1955), which considers the responsible physical mechanism as being vertical transport of ionization by electromagnetic forces combined with diffusion, moving the plasma upwards at the magnetic equator, with drift velocities up to 20 m/s on quiet days and considerably higher speeds under disturbed conditions, and across the magnetic field lines, subsequently diffusing down the field lines and forming ionization concentrations to the north and south of the magnetic equator.

2.4 Summary and Conclusions

The F region theory presented in this review has provided a first order description of F region phenomena. The processes which determine N(e) as a function of height and time may be summarized as follows (Rishbeth and Barron, 1960 and Rishbeth, 1967): The triggering solar radiation responsible for the F region ionization is principally that from 200 to 911 A. The production rate (q) is found to be a maximum at the F1 region level, varying with solar cycle and solar zenith angle. The distribution of N(e) is

determined by equilibrium between production and loss and is given by $q \simeq \alpha N^2$ at the lower F region heights, and by $q = \beta N$ for those heights nearer the peak. Proceeding beyond the F1 layer, β is found to decrease faster than q and $N(N \simeq q/\beta)$ increases rapidly upwards to the F2 peak where plasma diffusion dominates and N(e) begins to decline. The peak of N(e) is found near the level where the loss rate β becomes equal to the diffusion rate $d = D/H^2$. While beyond the peak, the N(e) distribution is governed by diffusion and the plasma assumes a diffusive equilibrium exponential distribution.

CHAPTER III

REVIEW OF PREVIOUS STUDIES

3.1 Geomagnetic Storms

Most notable of the characteristics of magnetic storms is a simultaneous depression of the magnetic field strength in low and middle latitudes. Superimposed on this systematic depression of the field strength are both regular and irregular variations of constantly changing magnitude and period that produce distinct perturbations in magnetogram traces, depending upon the location of the recording magnetic stations which are situated throughout the world. These complex storm variations may be resolved into constituent components; those possessing universal-time dependency and those of local-time dependency. The former component is called storm-time variation, indicated by Dst, and the latter is called disturbance-daily variation denoted by Ds.

Investigations conducted by Chapman and Bartels (1940) and Chapman (1956) describe the identifying characteristics that a magnetic storm undergoes in the course of its development and decay in terms of several distinct phases; denoted simply as the initial, main, and recovery phases in reference to a storm time which is reckoned from the commencement of the storm. Chapman (1935) identified upper atmospheric idealized current systems as being responsible for the universal-time Dst and local-time Ds, magnetic

storm components, the latter resulting from polar ionospheric currents and the former from current systems well beyond the ionosphere.

Most magnetic storms begin with an abrupt increase in the horizontal geomagnetic field component H in the low and middle latitudes. This abrupt beginning is known as the storm sudden commencement denoted simply as SC, and is usually complete within several minutes. Typical values of increase of H range from 20 to 30 gammas.

Subsequent to the abrupt commencement, the magnetic field remains above the pre-storm level for a period of time, typically 2 to 8 hours. This phase of the storm is identified as the initial phase.

The initial phase is followed by a large depression in H, constituting the main phase of the magnetic storm. The main phase displays depressions in H of 50 to 100 gammas and usually lasts from 12 to 24 hours in the low and temperate latitudes. These depressions greatly exceed the pre-storm value enhancement of H achieved during the initial phase. The minimum value of H in the main phase is generally attained several hours subsequent to the initial phase, proceeding to recover slowly to its pre-storm value.

This recovery of H from its minimal value reached during the main phase toward its pre-storm undisturbed level, progressing rapidly at first and more slowly later, is the decaying phase of the storm and is identified as the recovery phase.

Several conflicting theories have been proposed to describe magnetic storm phenomena. These suggested theories may be categorized as representing three very distinct schools of thought concerning the general theory of geomagnetic storms.

The predominant theory at present is that proposed by Chapman - Ferraro - Martyn (1931, 1932, 1933 and 1951) depicting the magnetic storm as being initiated by solar plasma impinging upon the geomagnetic field. The solar storm plasma is confronted by the geomagnetic field, forming a forbidden region or cavity where the geomagnetic pressure balances the impact pressure of the solar plasma. The rising of the geomagnetic field to meet the hydrodynamic pressure of the solar plasma is interpreted as being responsible for the SC (sudden commencement). The solar plasma, unable to penetrate the upper atmosphere due to the confronting pressure of the new compressed geomagnetic field, streams past the point of impact with the geomagnetic field and closes the cavity on the rear side of the earth, thereby completing a conducting circuit around the earth. This conducting region induces a "ring current" to flow from east to west, circling both hemispheres. The succeeding magnetic field generated by this westward ring current system depresses the geomagnetic field and is identified as being responsible for the main

phase of the magnetic storm. The subsequent progressive decay of the ring current is considered responsible for the recovery phase.

Suggesting the existence of a magnetic field inside the solar plasma and the subsequent generation of an electric field within the plasma due to the polarizing influence of motion of the ionized gas as it proceeds through space, Alfven (1955), in contrast to the Chapman - Ferraro - Martyn proposal, depicts the interaction of the weakly-ionized plasma in the combined plasma electric field and geomagnetic dipole field as initially leading to a counter-clockwise current system, identified with the SC, and subsequently, to a clockwise current system, identified with the main phase of the storm. Discrepancies concerning the excessive time delay, approximately eight hours, between the SC and the maximum of the main phase, and the location of the SC currents at rather removed distances from the earth, subject Alfven's proposal to judicious criticism.

Singer (1957) proposed that a solar stream perturbs the geomagnetic field at large distances, creating a "shockwave" in interplanetary space, preceeding the plasma stream. Part of the corpuscular stream is subsequently captured by the geomagnetic field and proceeds to drift gradually in a longitudinal direction in the magnetic field, positive ions drifting westward and negative ions

drifting eastward. This produces a net westward current, identified as the ring current responsible for the main phase decrease of the geomagnetic field.

Dessler and Parker (1959) and later Dessler, Hanson, and Parker (1961) were recent proponents of the "hydromagnetic theory" of magnetic storms. They suggested that during the initial phase precipitated by the increased solar plasma pressure upon the geomagnetic field, instability, generated by the impact of the solar plasma, causes small plasma clouds to become imbedded in the geomagnetic field. These plasam cloud particles then diffuse into the geomagnetic field to within 3 to 5 earth radii and form a belt of trapped particles consisting chiefly of protons and electrons. The trapped protons exert stresses within the geomagnetic field, primarily due to centrifugal force, and as a consequence, hydromagnetic waves are propagated to the ground surface. This, in turn, is responsible for the depression of the geomagnetic field during the main phase, and the hydromagnetic waves generated upon impact of the solar plasma with the geomagnetic field are then identified as the causative mechanism precipitating the SC. The impounded protons later transfer their energy to the neutral hydrogen, thus relieving the stresses within the geomagnetic field. This relief of stresses can be identified as the recovery phase.

Piddington (1960) advanced a geomagnetic storm theory in which the lines of force of the geomagnetic field

constitute a "tail" on the dark side of the earth which become connected with the passing solar stream and are withdrawn away from the sun due to the momentum of the ions in the stream, resulting in a decrease in the geomagnetic field. Furthermore, Piddington considered the detected geomagnetic disturbances to have their sources in lower ionospheric current systems, in turn sustained by related current systems situated in the region of interaction between the solar and terrestrial plasma.

3.2 Ionospheric Storm Phenomena

Disturbances and aurorae in the F region of the ionosphere associated with geomagnetic storms are the most pronounced and colorful manifestation of "ionospheric storms", any departure of ionospheric parameters from the usual state being defined as an ionospheric storm. Since the upper atmospheric current systems responsible for magnetic disturbances are situated in the ionosphere, an investigation of the ionosphere during storm conditions should yield very useful information concerning the physical mechanisms responsible for geomagnetic storms. For instance, aurorae provide unique evidence of particles precipatating from the magnetosphere and interacting with the ionosphere.

Important systematic features of ionospheric storms have been derived on the basis of statistical studies conducted by Appleton and Piggott (1952), Martyn (1953), Matsushita (1953, 1959), Obayashi (1954), Sato (1956, 1957),

Sinno (1954, 1955), and Somayajulu (1963) clearly demonstrating that the F2 region is particularly affected during magnetic storms. Principle among these features is the marked dependence, displayed by magnetic storm effects on the F2 region, upon the geographic latitude, season, and local time. There subsequently commenced a detailed investigation by research groups throughout the world of pertinent ionospheric parameters during magnetic storm conditions; specifically, changes in foF2, h'F2, and hp (the critical frequency, the virtual height of the F2 layer, and the height of the peak of the layer) for different latitudes and local times and for all the principle seasons of the year. These in-depth studies revealed certain conclusive systematic responses of the ionosphere to geomagnetic storms: namely, that at high latitudes a marked depression of foF2 (peak electron density) takes place, the maximum depression being centered near local noon; at middle latitudes there may be a depression or an increase in foF2 depending upon the local time and season; at low and near-equatorial latitudes, a depression is a rarity and a definite increase in foF2 for all seasons is usually the case. The general trend in h'F2 was found to be upward in most cases, being less pronounced at the near-equatorial latitudes (Somayajulu, 1960). However, it should be realized that this height parameter experiences excessive group retardation effects due to lower ionospheric regions, as is the predominant case in the intermediate and

high latitudes during magnetic storms, resulting in disturbingly large differences in hp of the F2 region and the respective true heights. Hence it is unreliable for deducing height changes during magnetic storms.

Initiating world-wide studies of the morphology of ionospheric storms were Appleton and Piggott (1952) and later, Martyn (1953) and Matsushita (1959). From these studies it was revealed that the correlation between foF2 and the responsible magnetic disturbance varied in magnitude and sign depending upon the respective station location, and that this correlation varied with the respective seasons.

In a more sophisticated treatment of ionospheric storms, Martyn (1953) studying the variations in the heights and densities of the storm affected ionospheric regions deduced that the ionospheric disturbance variation consists of two components; the storm time variation Dst, which is the medial variation over all longitudes and hence of all local times at a particular latitude and is reckoned with respect to storm time (the SC of a geomagnetic storm), and the disturbance diurnal variation Ds, the diurnally varying component or disturbance local-time inequality.

Fukushima and Hayasi (1952) from a study of Dst (foF2) variations concluded that Dst (foF2) displays a seasonal dependence and that the intermediate latitude F2 region electron densities (foF2) decrease in local summer and increase in local winter during magnetic disturbances.

Matsushita (1959), from a systematic study of data acquired from ionospheric stations throughout the world during numerous ionospheric storms occurring in the period 1946-1955, detected pronounced dependence of ionospheric disturbances upon latitudes and storm time. Matsushita found that the most severe depressions in N(e) (and hence foF2) occur within 20 and 40 hours storm time in dip latitudes of 45^{o} and greater, while in intermediate latitudes only a mild depression results, and in the near-equatorial regions, a definite increase is noticed. Initial increases in N(e) were detected in all zones except in the lowest latitudes within the first 9 hours of the storm commencement. In addition to storm time variations, there were discovered marked local time variations; specifically, the time of maximum depression of NmF2.

Most recently, with the availability of satellite observations, detailed information has been furnished on the storm-time behavior of the topside ionosphere during magnetic disturbances. Wilmore and Henderson (1965) report increases in topside N(e) during periods of magnetic disturbances at high latitudes, with the gradual progression of these high latitude N(e) enhancements toward the near-equatorial latitudes as the storm intensifies. Sayers (1964) reports rather large increases in topside electron densities for moderately disturbed conditions at the high latitudes. Both increases and decreases in N(e) have been indicated by King et al. (1967), the particular response

depending upon the specific latitude affected. Thomas and Venebles (1966) purport studies indicating that the change in NmF2 at any mid-latitude station is determined by the phase of the magnetic storm. Reddy, Brace, and Findlay (1967) indicate strong increases of N(e) at middle and high latitudes on the dayside, with weaker increases on the nightside. Matsushita (1959, 1963) reported on the basis of an intensive statistical analysis of world-wide ionospheric data, that the subpeak electron content decreases at middle and high latitudes while increasing at near-equatorial latitudes. From satellite observations (Odishaw, 1964), it has become apparent that the topside total electron content during a magnetic storm behaves in a similar manner. However, enhancements and depressions of topside ionization were reported by Titheridge and Andrews (1967) and by Hibberd and Ross (1967), from studies of total electron content measurements, to depend most heavily upon the respective phase of a magnetic storm. Most recently, Bauer and Krishnamurthy (1967), from an analysis of topside sounder observations, have reported both enhancements and depletions of topside ionization, depending upon the phase of the magnetic storm.

These results have been interpreted in disturbed F region theory as representing real increases and decreases in the total electron content of the F region under storm conditions and not merely a redistribution of ionization. Martyn (1953) has theorized that vertical drift motions of

the F region electrons, resulting from the interaction of the geomagnetic field with the magnetic storm generated electric field, would contribute significantly to prominent diurnal variations in the disturbed F region. In contrast, Matsuura (1963) and Yonezawa (1963) propose considerable temperature changes induced by geomagnetic storms as being responsible for storm-time variations in the F region. They proposed that N(e) production and loss rates and the diffusion rate would be affected by substantial increases in the F region temperatures, thereby producing extensive electron density variations.

However, the theory put forth by Matsuura and Yonezawa conflicts with recent findings reported by Titheridge and Andrews (1967) in a study of continuous records of the total electron content of the ionosphere derived from a geostationary satellite. Titheridge and Andrews, investigating the rather abnormal increase suffered by the storm-time mean scale height, considered an initial, rapid heating of the upper ionosphere by magnetic activity to be responsible. However, an increase of $500^{o}K$ would be required to achieve this change in the mean scale height and such mean plasma temperature changes are unconfirmed by incoherent back-scatter measurements conducted by Evans (1965). Instead, these severe changes in the mean scale height were interpreted as implying a large influx of electrons from the upper ionosphere, produced by a world-wide movement of ionization to lower field lines.

Subsequent severe reduction of the mean scale height on the following day was interpreted as indicative of increased mixing of the ionosphere, producing an increase in the mean ionic mass due to the presence of more neutral molecules in the F region. In support of this scheme, Reddy, Brace, and Findlay (1967) in an investigation of the storm-time response of the ionosphere at 640 kilometers, concluded that the storm-time enhancement of N(e) may be achieved in terms of a thermal expansion of the neutral atmosphere which lifts the whole of the ionosphere, thereby increasing N(e) at a particular, constant altitude; while a reduction in Te, ionospheric electron temperature, at temperate and low latitudes is interpreted as indicating both increased collisional cooling to an expanded neutral atmosphere and a reduction in the escape flux of photo-electrons responsible for additional heating of the upper F region.

Supporting the theory of Reddy, Brace, and Findlay (1967) are the more recent findings reported by Ondoh (1967) in a statistical investigation of the change in electron density and plasma temperature in the topside ionosphere during magnetic disturbances, employing Alouette I electron density and plasma scale height data. Ondoh attributes the increase in electron density in the auroral and middle latitudes to a lifting of the topside ionization initiated by the thermal expansion of the neutral atmosphere due to accompanying temperature enhancements. Further

analysis of plasma scale heights during disturbed periods reveal an enhancement of the plasma temperature, being larger in the nighttime than in the daytime at high and middle latitudes.

In contrast to the findings of Reddy, Brace, and Findlay (1967) are those of Rao (1968) in an analysis of incoherent backscatter measurements of the F region electron concentrations and electron and ion temperatures Te and Ti respectively, conducted at Arecibo during the magnetic storm of June 15 and 16, 1965. Principle responses of the topside ionosphere to the magnetic storm include enhancements of electron densities and nighttime plasma scale heights by a factor of 1.5 to 2.0 and 2.0 to 3.0, respectively. The electron temperatures under disturbed conditions were found to be 200-300^{o}K higher than the quiet day values during nighttime, while the daytime changes were within the diurnal variations. The diurnal variation of the disturbed Ti displays increased temperatures near 225 km and 300 km and depressed temperatures, compared to quiet-day conditions, near 375 km and 450 km height levels; indicating that under disturbed conditions the ion temperature is coupled to the neutral temperature to a greater height level than during quiet conditions, suggesting increased neutral particle densities during the magnetic disturbance. Rao (1968) further proposes that the large increase in the light ion concentration in the topside ionosphere and concurrent substantial Te

enhancements both imply a storm-time increase in the downward diffusion of plasma from the protonosphere to the nighttime F region, the causative mechanism being the interchange of tubes of force in the magnetosphere during magnetic disturbances as initially postulated by Cole (1964).

Recent topside sounder studies conducted by Bauer and Krishnamurthy (1967) of Alouette I data on the great magnetic storm of April 17 and 18, 1965, indicate that both enhancements and depletions of topside ionization can be realized depending upon the phase of the magnetic storm. Specifically, throughout the initial (positive) phase of the storm, topside ionization is enhanced - compression of the dayside magnetosphere, leading to a downward transport of ionization along the field tubes, being the responsible mechanism. Bauer and Krishnamurthy refuse the possibility of heating effects as precipitating the increase in topside N(e) for there is negligible change in scale heights during the initial phase, implying the absence of pronounced heating effects. Furthermore, during the storm main and recovery phase, the inner magnetosphere is inflated, resulting in the expansion of field tubes due to the presence of the high density ring current plasma, causing an upward flux of ionization from the topside ionosphere along the connecting field tubes, resulting in a subsequent reduction of ionospheric electron densities. Concurrent analysis of accompanying storm-time scale

heights suggest that the mean ionic mass is higher on storm days than quiet days, indicating that the lighter ions (protons) are substantially depleted.

3.3 Ionospheric Storm Theories

Recognition of ionospheric disturbances being initiated by magnetic disturbances is very detailed, but the physical mechanism which links the two phenomena is very controversial and as of yet, there is no satisfactory theory which completely describes the major features of ionospheric storms in the F region. This is due in large part to the extreme complexity attributable to the formation of the F region even under quiet ionospheric conditions. Although the theories of ionospheric storms are still at a speculative stage, several responsible theories, consistent with our recent knowledge of related geophysical phenomena, have been proposed to explicate the observed physical changes occurring during ionospheric disturbances. These are, respectively:

(1) Thermal Expansion Theory
(2) Temperature Dependence of Loss and Diffusion Coefficients Theory
(3) Recombination Theory
(4) Electromagnetic Drift Theory

(1) Thermal Expansion Theory: This theory was first proposed by Meek (1953), Nagata and Oguti (1953), and Kamiyama (1956) where it was maintained that solar corpuscles, responsible for the ionospheric disturbance, precipitated into the auroral regions generating heat causing the subsequent thermal expansion of the upper

atmosphere and producing a depression of electron densities in the auroral zone. From observations of drag acting on artificial satellites, it is known that the temperature of the neutral atmosphere increases during magnetic disturbances (Knecht, 1959) and the resulting thermal expansion would certainly increase the thickness of the F2 layer, but the effects on NmF2 are most likely to be rather small; also, the thermal expansion would cause hmF2 to increase, but this has not been detected. Further inadequacies of this theory include its failure to explain the occurrence of disturbances in middle and low latitudes and the repetition of disturbance diurnal variations.

(2) Temperature Dependence of Loss and Diffusion Coefficients Theory: From studies of satellite drag data, Jacchia (1961) and Groves (1961) have inferred that there is a general heating of the upper atmosphere during geomagnetic storms, causing considerable enhancement of temperatures in the F region. Yonezawa (1963), from a study of changes in hmF2 and NmF2 during severe magnetic storms, maintains in his theory that the rate of chemical reactions of certain pertinent photochemical processes, responsible for affecting substantial changes in electron equilibrium under disturbed conditions, are very sensitive to temperature change. Therefore, Yonezawa interprets the reduction of the peak electron density as a manifestation of an increased electron loss rate effected by enhanced F region temperatures during disturbed conditions.

Matsuura (1963), in a study of an intense ionospheric storm, demonstrated that the dominant processes controlling electron density variations during storm conditions are those of electron loss and ambipolar diffusion. Matsuura maintained, upon numerically solving the electron density continuity equation using functional relations expressing the dependence of electron loss and diffusion upon temperature, that only a marginal change of temperature is required to affect substantial changes in electron loss and diffusion rates, thereby yielding the observed variations in electron densities. The effect of temperature variation on electron loss (l) and diffusion (D) was found to be remarkable - a temperature rise yielding an increase in l, due to an increase in molecular ionospheric density, and a decrease in D, due to an increase in the total ionospheric density.

(3) Recombination Theory: Seaton (1956) suggested a chemical mechanism as being responsible for F region changes during magnetic storms. Solar radiation, ionizing N_2 and O, produces an ionization maximum at 160 km identified as the F_1 peak. The N_2^+ ions quickly recombine with electrons by a dissociative recombination process. The O^+ ions in turn precipitate a loss of electrons by a combination of a radiative recombination process and dissociative recombination processes as given below:

$$O + h\nu = O^+ + e \qquad (3.1)$$

$$O^+ + O_2 = O + O_2^+ \qquad (3.2)$$

$$O_2^+ + e = O + O \qquad (3.3)$$

The recombination rate of the above recombination processes is controlled by the prevailing O_2 density. If the density of O_2 is fractional relative to that of O, the ionizable constituent, then the reaction rate is firmly controlled by the O_2 population and is proportional to a βN law, where N is the electron density. However, if the O_2 population, instead of being a minority, is now comparable to that of O, the recombination rate is proportional to an αN^2 law which is dominant in the lower F region of the quiet ionosphere (normally the loss rate of electrons decreases with height). Seaton proposed that the principle mode of electron loss in the F region is through dissociative recombination with O_2^+ as depicted in equation (3.3). Thus, the rate of removal of electrons in the F region becomes critically dependent upon the concentration of O_2 available for the charge-transfer reaction (3.2). The basis of Seaton's proposal is that during storm conditions the upward vertical transport of O_2 increases, possibly by turbulance (under these conditions the βN law becomes an αN^2 law), leading to an increased rate of recombination and causing considerable reduction in the upper F region ionization. The attractive feature of this theory is that is predicts a reduction in N(e)

throughout the F region rather than merely a redistribution of ionization, and thus complies with recent findings by the topside sounder satellite, Alouette I, which clearly indicated that N(e) is reduced at all levels intermediate of the F2 peak and the height of the satellite (1000 km).

(4) Electromagnetic Drift Theory: The principle theoretical groundwork was initially labored by Martyn (1953) and has since been refined by other workers, notably Maeda (1955), Hirono (1955), and Sato (1957). This electrodynamic mechanism as proposed by Martyn, describing the behavior of the F region during storm conditions, links the F region storm phenomena directly to the Ds component of the current system generated by the geomagnetic disturbance. His theory proposes that the existence of the Ds current system necessitates the existence of a corresponding driving electric field. The combined interaction of this electric field with the geomagnetic field will cause the F region ionization to acquire a velocity in the direction of $\overline{E} \times \overline{B}$, resulting in a vertical drift component which subsequently drives the random drift motions of the electrons leading to a redistribution of ionization. The consequent equilibrium distribution of electron density can be determined by solving the continuity equation using the estimated vertical drift velocities and an assumed atmospheric model of electron production and loss rates. Thus, Martyn has proposed that vertical drift motions of electrons, resulting from the interaction of the

geomagnetic field with the electrostatic field identified with ionospheric storm-time current play a dominant role in the behavior of the F region during geomagnetic storms. Quantitative results demonstrate satisfactory concurrence with observation as concerns changes in NmF2 and h'(f) at midlatitudes; and results arrived at by Maeda and Sato (1959) yield reasonable agreement between calculated and observed Ds variations in the middle and low latitudes. In addition, Martyn's theory has been successfully utilized by Maeda (1 53) and Sato (1956, 1957) in describing the latitudinal and seasonal variations of F2 ionization. However, as attractive as the drift theory may appear, major difficulties become evident when attempting to apply accepted ionospheric parameters to predict the observed storm-time electron density variations; specifically, the inability of this theory to accurately describe the typical effect of storms, a reduction in NmF2 accompanied by an increase in its height, is a major and crucial shortcoming. Nevertheless, the principle feature of the drift theory remains - it provides a responsible description of the variation of the disturbed ionosphere, as precipitated by the ionospheric Ds current system, with respect to local time and latitude. Thus, in this regard, the importance and existence of the electrodynamical drift theory is an inescapable consequence of the correlation between ionospheric and geomagnetic Ds variations.

Dst variations in low latitudes, responsible for producing an increase in the electron density during storms, as yet, remains unexplained. Here, the diffusion (Rishbeth, Van Zandt, and Norton, 1966) of electrons along the near-horizontal geomagnetic field lines causes considerable distortion of the electron density distribution (Obayashi, 1964). However, Yonezawa (Odishaw, 1964) has gleaned a promising idea, interpreting the low latitude storm effects in terms of a positive temperature change. Because the height of the F2 peak at the near-equatorial latitudes is particularly high (400 to 500 km), the molecular population there is extremely diminished. Hence, Yonezawa proposes, the dominating electron loss mechanism is that of a radiative recombination process, given as follows:

$$O^+ + e = O + h\nu$$

The corresponding recombination coefficient is inversely temperature sensitive. Thus, increasing ionospheric temperatures will precipitate increases in the F2 peak electron densities, while reductions in electron densities may simultaneously prevail at intermediate and lower heights as in the middle latitudes, due to enhanced electron loss rates.

CHAPTER IV

IONOGRAM REDUCTION AND DATA PROCESSING TECHNIQUES

The processing of large volumes of data was necessitated in attaining the raw data in its final presentable form. Use was made of the Alouette I topside sounder satellite for a detailed analysis of the ionosphere under disturbed conditions. The Alouette I sounder satellite, built by the Defense Research Board of Canada, initiated topside soundings of the upper ionosphere with its successful launching by the National Aeronautics and Space Administration (NASA) on September 29, 1962, into a very nearly circular orbit having an altitude of roughly 1000 km and an inclination of 80.1 degrees. The sounder consists primarily of a variable frequency pulsed radar contained in a satellite which records the virtual depths of reflection (h') from radio pulses vertically incident on the topside ionosphere, located below the satellite, as a function of frequency (f). The resulting h'(f) data, when displayed on photographic film or paper, is then denoted as an ionogram (Figure 4.1). The variable frequency sounder sweeps from 0.5 to 11.5 megacycles in 18 second intervals, during which time the satellite progresses 120 km along its 1000 km circular trajectory, thus providing approximately a single ionogram per degree of latitude. From the Alouette I sounder satellite latitudinal

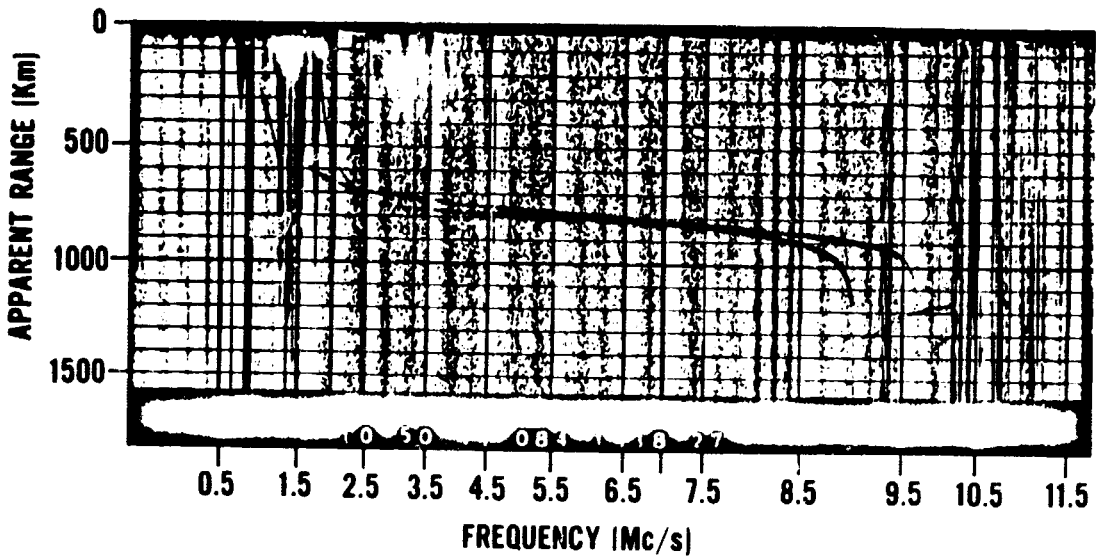

REPRESENTATIVE IONOGRAM FROM ALOUETTE I TOPSIDE SOUNDER SATELLITE

FIGURE 4.1

cross-sections of the ionization distribution of the topside ionosphere can then be constructed from the proper combination of consecutive N(h) profiles, analytically derived from topside ionograms.

Some of the ionograms recorded during the storms were of rather poor quality so that at times, latitudinal coverage was inadequate; thereby causing large gaps in the latitudinal variations of electron densities and vertical scale heights. Fusion of the traces at the low frequency spectrum of the ionograms caused considerable difficulty in their reduction. This is due, for the most part, to severely low densities, whereby the hybrid, F_{xs}, and gyrofrequency are subsequently very close and hence, quite difficult to distinguish.

Great care was consequently given to the selection of a suitable data reduction technique. Imperative in the selection of such a technique was the capability of more precisely reducing the typical well-defined ionograms to N-h profiles and yet, at the same time, remain particularly sensitive to rather severe discontinuities in the h'(f) profiles, representative of storm-time conditions, so that the rather poorly defined ionograms may still be utilized. Rapid changes of h' with frequency can severely tax the capability of many computer techniques to deduce a representative profile. With a suitable technique though,

many "poor" ionograms, typical of disturbed ionospheric conditions, which previously may have been unanalyzable, yield valuable and meaningful N-h profiles.

Consideration of two very capable computer reduction techniques was conducted: J. R. Doupnik's (1965) technique employing laminations parabolic in log fn and containing an iterative scheme compensating for the variation of fh with height, and that of Jackson (1967) employing a parabolic in log N lamination technique and an iterative scheme whereby successive true height profile calculations agree to within 0.01 km.

Comparison of the two ionogram reduction techniques consisted of presenting a number of h'(f) curves, representative of daytime and nighttime ionograms, under both quiet and disturbed ionospheric conditions, as input data to the respective computer programs. From subsequent corresponding N(h) profiles deduced using the different techniques, a comparison can be drawn and the relative accuracy of the techniques determined. Comparison of the respective N(h) profiles yielded a congruence of ± 10 kilometers, which is well within the minimal range of inaccuracies inherent in scaling errors and reduction techniques (Table I).

Before a complete and judicious comparison can be concluded, a discussion of the measure of scaling and calibration errors involved in the reduction is most necessary at this point.

Table I

Comparison of J. E. Jackson and J. R. Doupnik Ionogram Reduction Methods Using a Nighttime Ionogram Under Magnetically Disturbed Conditions.

Date		Time	HS	FHS	Dip at Satellite	
June 17, 1965		0025 LMT	1000 km	0.7700	29.48	
h'(km)	fx(mc/s)	h(km)	$N(e)\cdot 10^4(cm^{-3})$ J. E. Jackson		h(km)	$N(e)\cdot 10^4(cm^{-3})$ J. R. Doupnik
00.0	1.318	1000.0	1.2702		1000.0	1.3797
32.0	1.341	992.3	1.3364		993.7	1.3481
100.1	1.364	980.6	1.3956		984.7	1.4237
144.1	1.387	961.8	1.5241		964.4	1.5926
184.1	1.410	922.8	1.6596		924.2	1.7472
444.3	1.461	888.2	1.7992		891.8	1.9224
563.6	1.514	847.5	1.9439		852.3	2.2781
663.6	1.566	808.7	2.0878		815.9	2.4892
809.5	1.619	741.7	2.3894		748.2	2.9342
876.2	1.670	678.6	2.7306		687.3	3.6405
967.9	1.770	618.7	3.1312		627.4	4.0672
1031.4	1.875	571.2	3.5160		580.1	4.7792
1075.4	1.989	524.9	3.9678		532.3	5.1072
1103.8	2.091	449.4	4.9267		457.5	6.1371
1125.1	2.203	339.8	5.9341		396.7	7.0477
1154.9	2.418	337.5	7.0777		343.4	8.2213
1176.1	2.623	291.8	8.3343		296.7	9.4482
1197.4	2.833	251.9	9.6922		255.8	12.833
1214.4	3.044	200.5	11.867		205.2	13.713
1231.4	3.254	169.4	13.407		174.7	14.771
1279.6	3.761	151.0	14.419		157.4	15.537

There are three prime sources of error inherent in the processing of ionograms: that due to the instrumentation, such as the satellite and ground telemetry stations, that involved in the scaling of the ionograms, and lastly, that produced in the conversion of the virtual depths (h'(f)) to real height profiles.

Discussion of the errors arising from the instrumentation in the reduction of ionograms cannot be very detailed due to lack of information, at present, from responsible sources concerning the design of satellite instrumentation and telemetry systems, the processing of magnetic tape to photographic film, and related tasks.

However, the main errors in ionogram-to-true height profile conversion arises from inaccuracies in ionogram scaling and calibration. From exhaustive studies performed by Jackson (1967), Doupnik (1965), and J. O. Thomas (1965) concerning these inaccuracies introduced by uncertainities in the scaling of ionograms, it can be concluded that scaling inaccuracies of as much as $\pm$10 km in h'(f) can arise when ionograms are carefully, but rapidly, scaled; and even on high resolution ionograms, the scaling error introduced into the virtual heights is at least $\pm$5 kilometers when meticulously scaled. Therefore, normal variations of approximately $\pm$5 km are likely to occur in the resulting N-h profile as a consequence of scaling inaccuracies. Under the severe ionospheric conditions induced by magnetic storms, subsequent poor quality ionograms, subject to

scaling by electronic digitizing machines, primarily employed in concern of the rapid, yet accurate, reduction of vast quantities of topside ionograms, may yield scaling inaccuracies in h'(f) of 20 to 30 kilometers!

The relative accuracies (or inaccuracies) of the individual techniques developed by Jackson (1967) and Doupnik (1965) may be assessed by comparing the N-h profiles deduced by each technique from theoretical electron density profile models. From studies such as these, Jackson and Doupnik concluded of their techniques that the random inaccuracies contained in the derived N-h profiles, directly contributable to the conversion techniques, are less than 1 kilometer. In this respect, keeping in mind the magnitude of the scalling inaccuracies, both computer techniques were judged to be equally qualified for the analysis of ionograms under severe ionospheric conditions. However, use of a four point calibration scheme contained in Jackson's computerized ionogram reduction technique, yields a substantial reduction (10 to 15 km) in scaling inaccuracies. Consequently, it was decided to employ Jackson's computerized conversion technique for the systematic reduction and interpretation of disturbed day ionograms. In the very near future, a five point calibration technique (Jackson, private communication), compensating for the non-linearity of the frequency gridlines, as well as height gridlines, will contribute significantly to increased scaling accuracy.

Complementing the computerized ionogram reduction and conversion technique was a computerized plotting technique utilized for the predetermined logical selection and permanent display of ionization density contour datum. Considerable time was devoted to the formulation of a suitable computer program that would identify and isolate from topside ionogram data contained on magnetic tapes (namely, individual electron density profiles and related geophysical parameters), those densities and scale heights corresponding to specific altitudes of 300, 400, 500, 600, 700, 800, 900, and 1000 km for all sub-satellite latitudes as recorded in a given satellite pass. The computer then proceeded to dictate the generation of an appropriate data display grid for permanent display and identification, in a Calcomp Model 536 Plotter, the intended latitudinal variations of ionization densities and scale heights. Input data consisted of magnetic tapes bearing the desired electron density profiles and related geophysical datum, derived from disturbed day ionograms corresponding to a number of satellite passes. The computer then plotted the selected electron densities, and vertical and horizontal scale heights; thereby presenting in a concise and meaningful manner, the complex latitudinal variations of the desired ionospheric parameters. Hence, use of this computer technique greatly facilitated the analysis of the magnetic storms and the vast volumes of data accompanying them.

CHAPTER V

SUMMARY DESCRIPTION OF PRESENT INVESTIGATION

Topside sounder satellites provide consecutive measurements of N-h profiles, from which may be derived variations of N(e) and Hv which in turn yield measurements of temperature and composition. In that the behavior of the ionosphere is governed principally by the physical processes of ion production, recombination, vertical movement and plasma diffusion, it is of prime concern to derive from these measurements the characteristic parameters such as temperatures and densities and subsequently relate these to the controlling physical processes so that the precise processes responsible for changes in the ionosphere under disturbed conditions may be identified.

Five principle means of investigation were employed in analyzing an ionosphere subject to magnetically disturbed conditions. The first involved the study of latitudinal contours of electron densities at discrete fixed altitudes, ranging from 300 to 1000 kilometers, inclusive. Secondly, latitudinal variations of the scale height parameter Hv, the vertical distribution of electron densities, were considered in investigating the variations of the ion and electron temperatures (Ti and Te) and the mean ionic mass ($\overline{m}_i$). Horizontal scale height (Hs) calculations were utilized in investigating the fluctuations of Te and Ti and the mean ionic mass at the low and near-equatorial altitudes.

In the investigation of the upper ionosphere, it is usually assumed that the transport of charged particles is confined to the field lines under diffusive equilibrium. Therefore, under these conditions, the scale heights of the field-aligned plasma Hs, rather than the scale height of the vertical electron density Hv, is the physically meaningful parameter. Under the conditions of diffusive and thermal equilibrium along the field lines in a simple dipole field with no vertical or lateral gradients of Te and/or Ti, and Te = Ti, the formulation for Hs as derived by Chrandra and Goldberg (1964) is given:

$$\frac{\bar{m}_i g}{k(Te + Ti)} = -(\partial N/\partial r)/N + (\cot \phi / 2Nr)\ (\partial N/\partial \phi) \qquad (5.1)$$

$$= 1/Hs$$

and

$$Hv = - N/(\partial N/\partial r)\big|_{\phi = \text{constant}} \qquad (5.2)$$

where g is the acceleration due to gravity, k is Boltzman's constant, r is the radial geocentric distance, ϕ is the geomagnetic latitude, and N is the electron density.

From the latitudinal values of Ne, corresponding values of Hs were calculated using equation (5.1), and graphs then constructed of Hs versus dip latitude - the analysis of the

low latitude fluctuations of Te, Ti, and $\bar{m}_i$ being intended. However, in a preliminary analysis of Hs, it was found that this parameter was too severely sensitive to minute fluctuations in the raw $N(h, \phi)$ data, and it was consequently decided that manual smoothing of the $N(h, \phi)$ data, prior to the numerical calculations, was necessary. Consequent to the manual smoothing though, the Hs values were still rather irregular in their variations and yielded inconclusive results. Recourse was then directed to a study of the distribution along magnetic field lines to derive the behavior of the ionization distribution and scale height variation along these field lines during magnetically disturbed conditions. Utilization of a simple dipole model of the geomagnetic field was realized in deriving the field-aligned electron concentrations. The defining relation for the field lines in geomagnetic coordinates follows:

$$r/r_o = \cos^2\theta/\cos^2\theta_o \qquad (5.3)$$

where r_o is the geocentric radial distance and θ the geocentric latitude. The incremental distance of arc-length along the dipole field line defined by equation (5.3) is given:

$$ds = r_o/\cos^2\theta_o \sqrt{1 + 3\sin^2\theta} \cos\theta \, d\theta \qquad (5.4)$$

where s is measured along that particular line of force, as determined by a specified θ_o and radial distance r_o, from the geocentric plane to a particular latitude θ. Plots were then constructed of the latitudinal variation of field-aligned electron densities and of N(e) versus (s), the distance traversed on a dipole model field line. The validity of the dipole field representation is justified by the meaningfulness of the results deduced from this mode of investigation, and in this restricted sense, is a rather well-founded representation for the low latitudes (Rishbeth, 1966).

CHAPTER VI

RESULTS AND DISCUSSION

6.1 June 15, 1965 Storm Analysis

First and most sustained of the magnetic storms to be studied was the moderately severe magnetic storm commencing June 15, 1965 where the value of K_p was greater than 5 for a 24 hour period. The storm sudden commencement occurred at 1100 hours UT on 15 June, and the main phase was fully developed by 2300 UT on 16 June, values of K_p remaining inflated for the succeeding 2 days (Figure 6.1), attaining a maximum value of 7 on 16 June. The period of June 10-15, preceeding the storm, was unusually quiet with K_p remaining less than 2 in value. Thus, this magnetic storm becomes particularly suited for the study of changes induced in an undisturbed ionosphere by an unusually strong magnetic disturbance. June 13 was selected as the prestorm quiet control day and hence, is representative of an undisturbed ionosphere.

Figure 6.2 presents the foF2 variations during the June storm near the 75°W meridian from the ionospheric observations of Huancayo, Talara, Grand Bahama, and Ft. Belvoir. Ft. Belvoir and Grand Bahama stations depict the familiar mid-latitude depression of foF2 while the near-equatorial stations, Talara and Huancayo, display pronounced enhancements of foF2 on 16 and 17 June. The ionosphere seems to have fully recovered by 19 June.

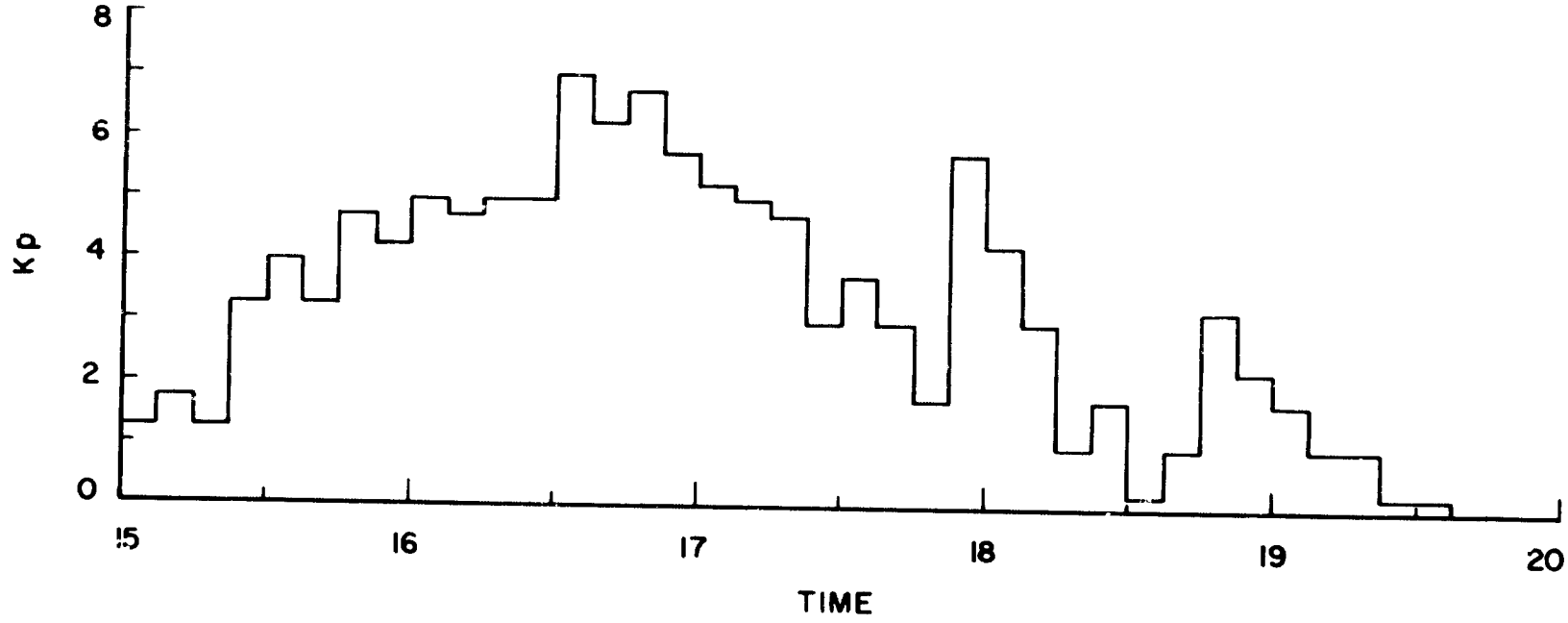

VARIATION OF Kp DURING JUNE 15, 1965 MAGNETIC STORM

FIGURE 6.1

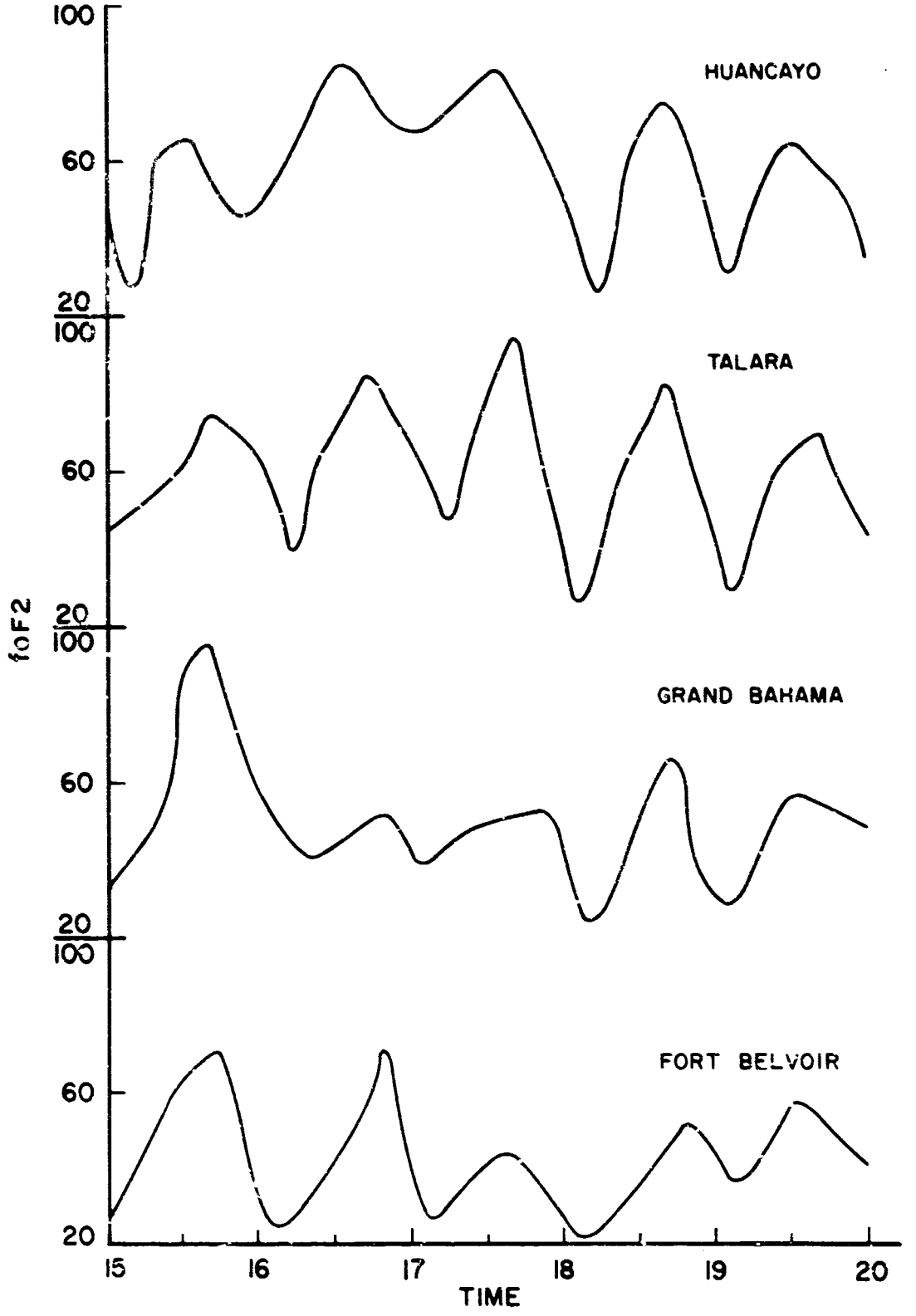

VARIATION OF foF2 DURING JUNE 15, 1965 MAGNETIC STORM

FIGURE 6.2

6.1.1 Electron Density Variations

Figure 6.3 presents the constants altitude contours of Ne for 13 June plotted as a function of dip latitude. Exceptionally prominent and readily distinguishable in Figure 6.3 is the appearance of the ionospheric equatorial anomaly, immediately identifiable by the trough in the electron density aligned with the magnetic dip equator, and also, by the crests of ionization situated at approximately -8^{o} and $+ 10^{o}$ dip latitude; with the anomaly no longer being visible at 700 km. The ionosphere displays a typical smoothly varying regular character, excepting some scattered small-scale irregularities which may probably be manifestations of longitudinal and/or time effects inherent in the topside ionosphere.

Inspection of Figure 6.4, which is the latitudinal plot for June 15, also a quiet day, shows the anomaly is still present. Figure 6.5 represents the latitudinal plot of N_e for the ionospherically disturbed day of 16 June. The transition from the initial phase to the main phase of the storm commenced at 0900 hours on this day. Referring to Figure 6.5, these contours are seen to be different from those of the quiet day 13 June. Unfortunately, the coverage did not extend beyond $5^{o}S$ into the northern hemisphere. Still, we can see that the N_e maximum at 400 km near -8^{o} on 13 June does not appear on 16 June, with the density increasing continuously with decreasing latitude. This is true for the N_e contours for the

remaining height levels. Thus, the contours of 16 June indicate that either the near-equatorial peaks are closer than 5^{o} from the magnetic equator or that they have been replaced by a single peak. There is also noticeable a marked ionization trough situated at -28.0^{o} dip latitude with increases in ionization developing below -30^{o}. Notice in particular, that the ionization enhancements are higher at the lower heights, namely 300 and 400 km.

Preliminary examination of Figure 6.6 corresponding to June 17 near local noon, reveals the disappearance of the anomaly with a single more pronounced crest of ionization located at the magnetic equator in its place. The equatorial maximum possesses a marked symmetry about the magnetic equator and displays a monotonic decrease with latitudes, the decrease being less steep at greater altitudes. We also notice that N_e at 400 km at the magnetic equator has increased over the pre-storm value due to the formation of a single peak at the magnetic equator wnile at the location of the pre-storm peaks the densities appear to be depressed. The density contour at 500 km does not show any appreciable change. For greater heights, the densities have increased at all levels.

Figure 6.7 refers to the N_e distribution on 18 June corresponding to the recovery phase of the magnetic storm. Referring to Figure 6.2, we notice that on this day foF2 is also recovering. Readily noticeable from the N_e contours of Figure 6.7 is the recovery of the equatorial anomaly

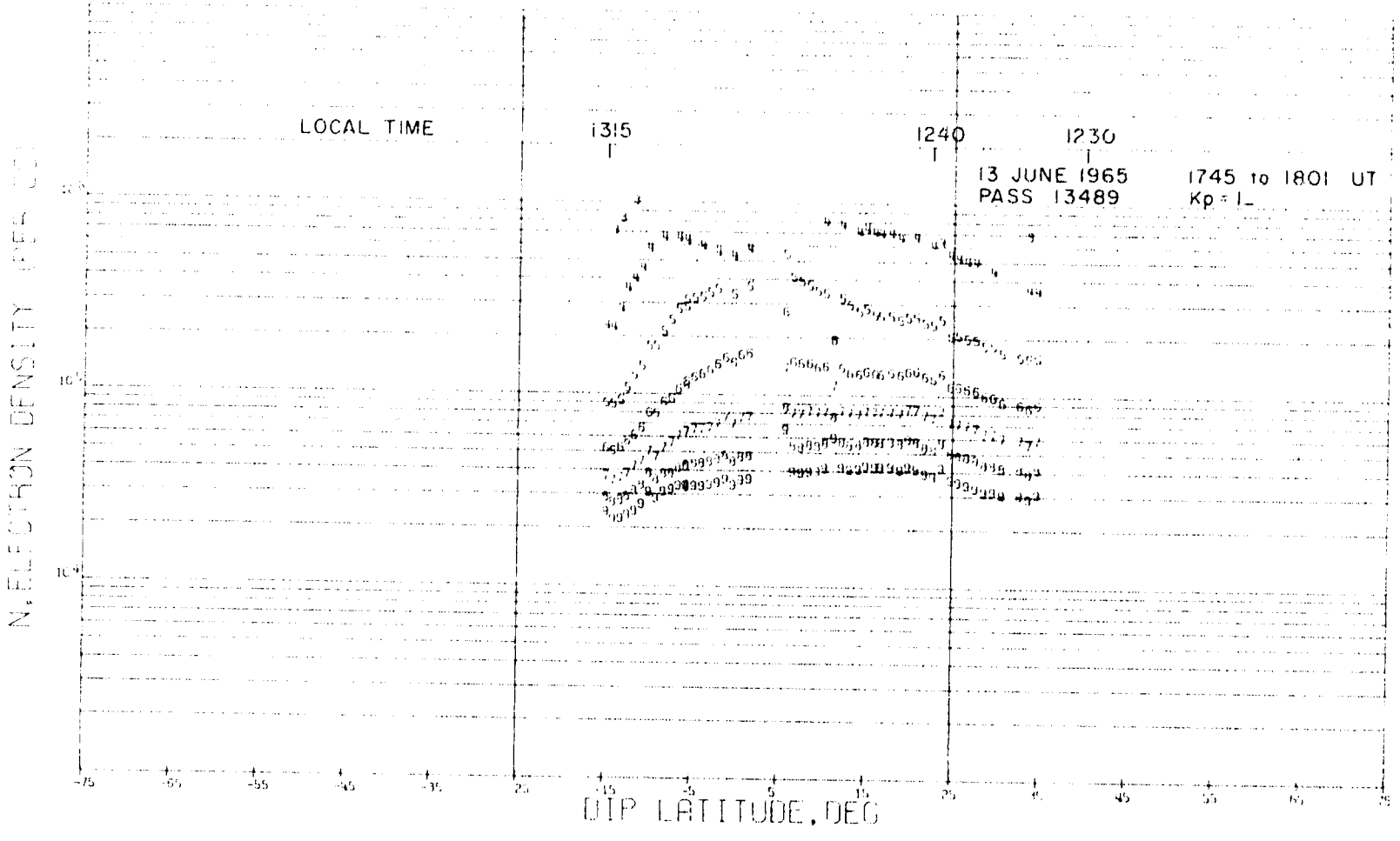

LATITUDINAL VARIATIONS OF N(e` ON JUNE 13, 1965

FIGURE 6.3

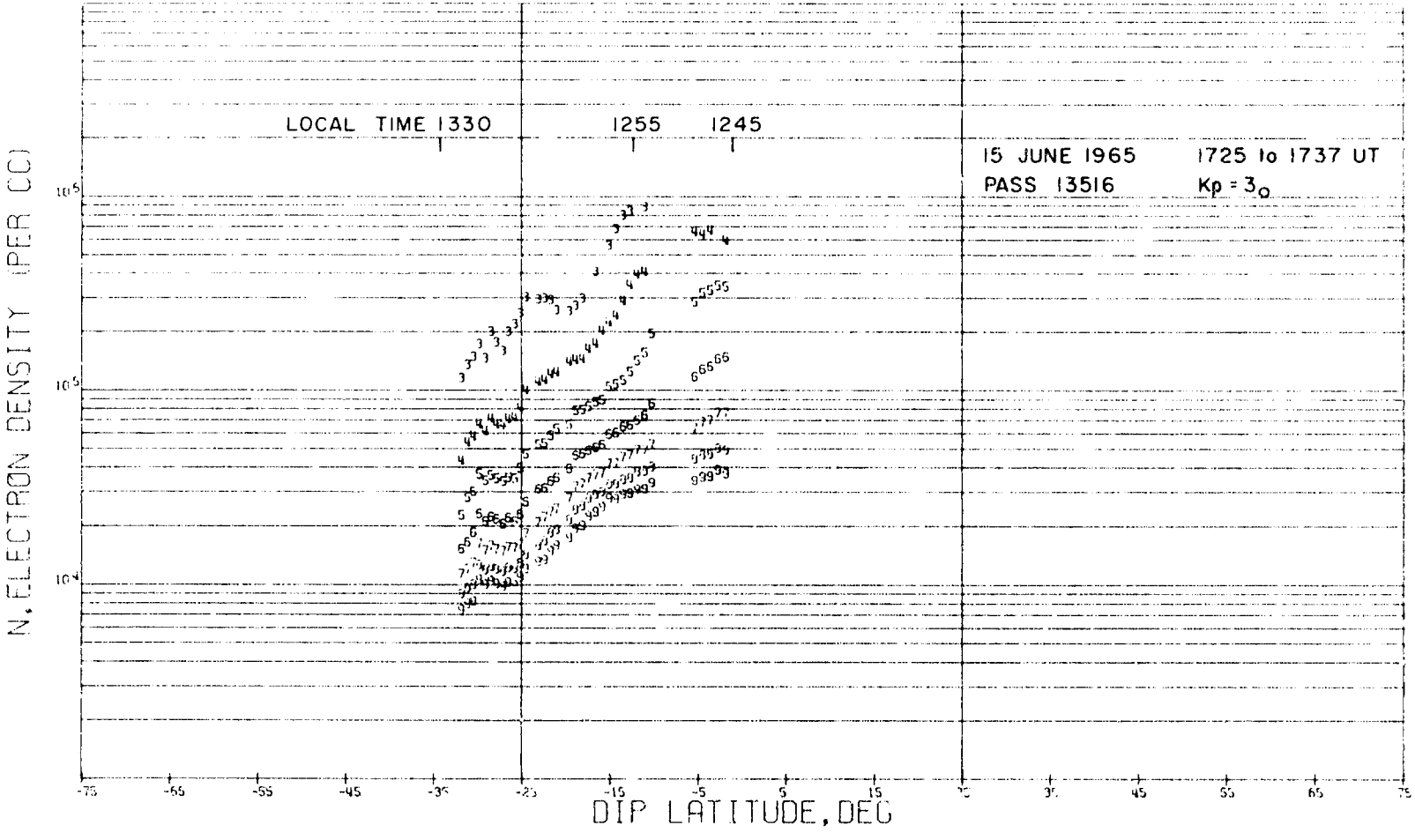

LATITUDINAL VARIATIONS OF N(e) ON JUNE 15, 1965

FIGURE 3.4

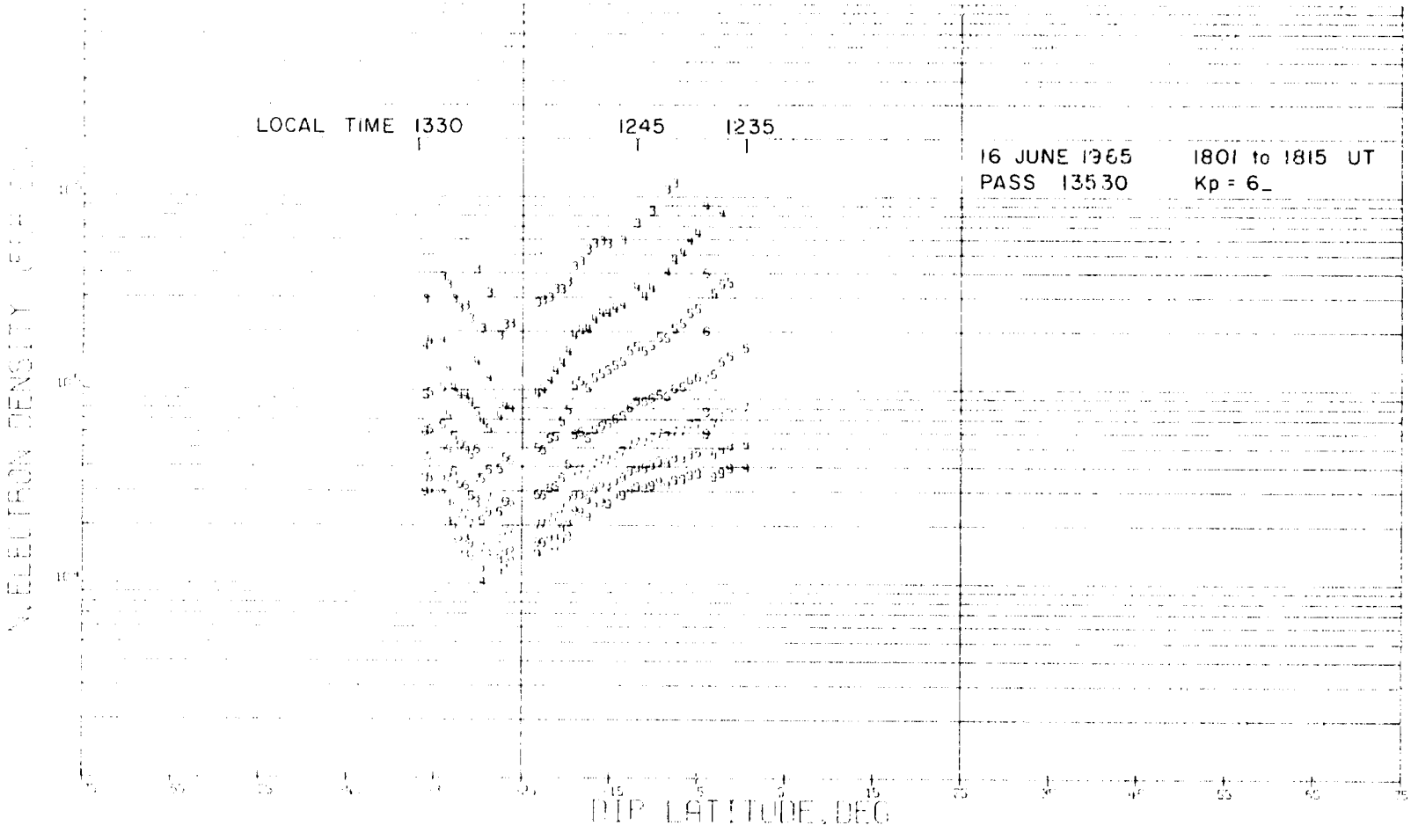

LATITUDINAL VARIATIONS OF N(e) ON JUNE 16, 1965

FIGURE 6.5

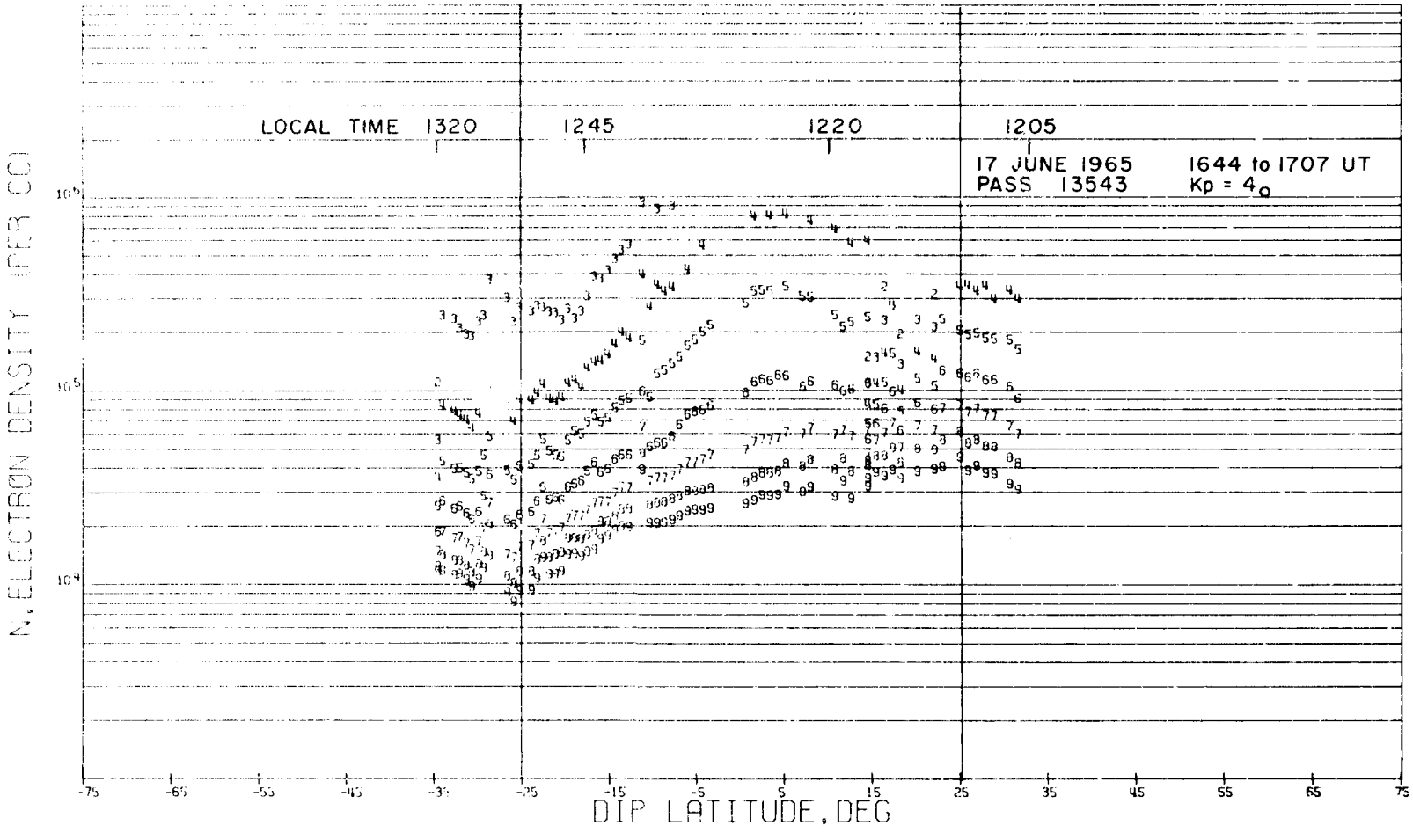

LATITUDINAL VARIATIONS OF N(e) ON JUNE 17, 1965

FIGURE 6.6

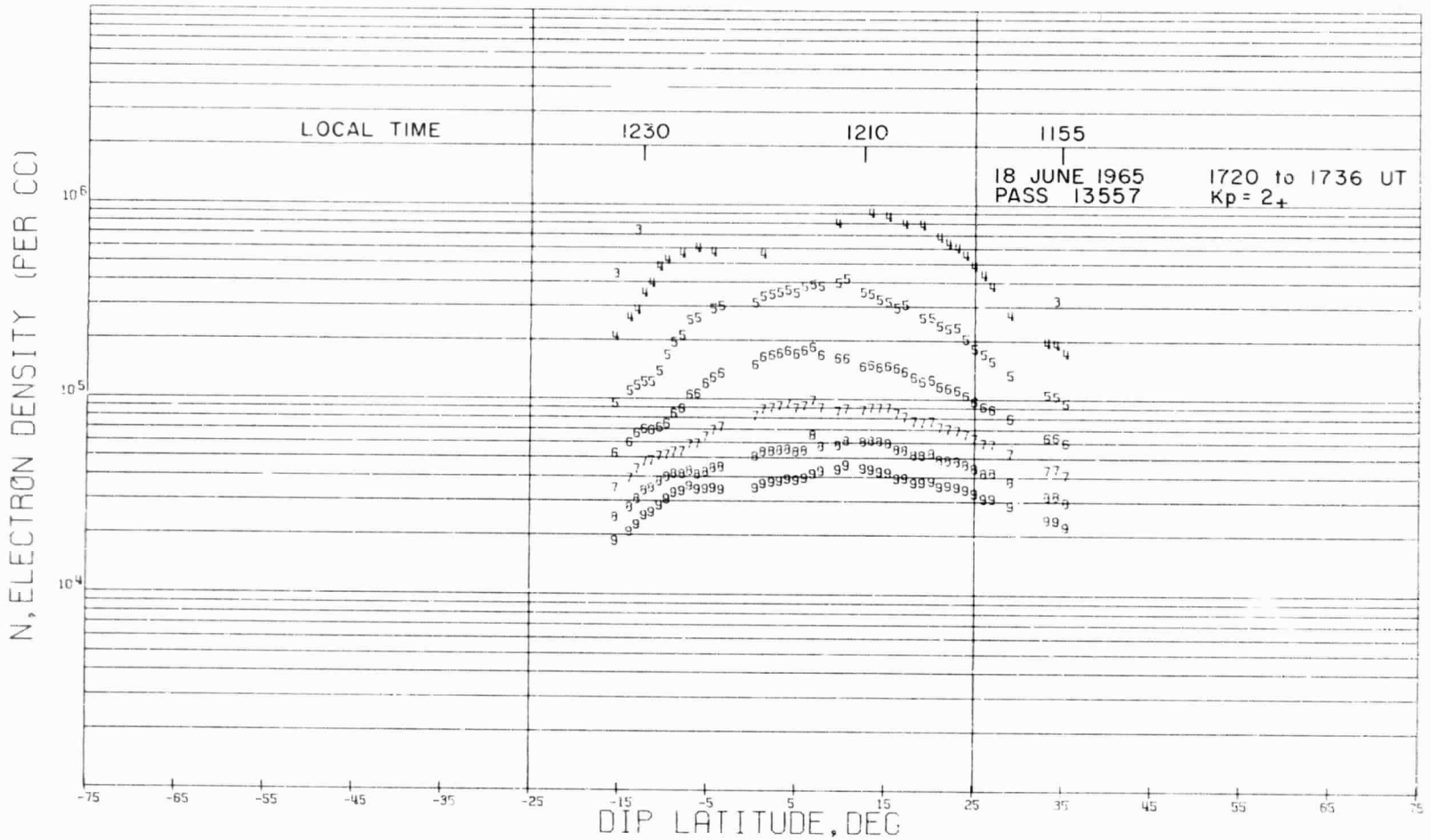

LATITUDINAL VARIATIONS OF N(e) ON JUNE 18, 1965

FIGURE 6.7

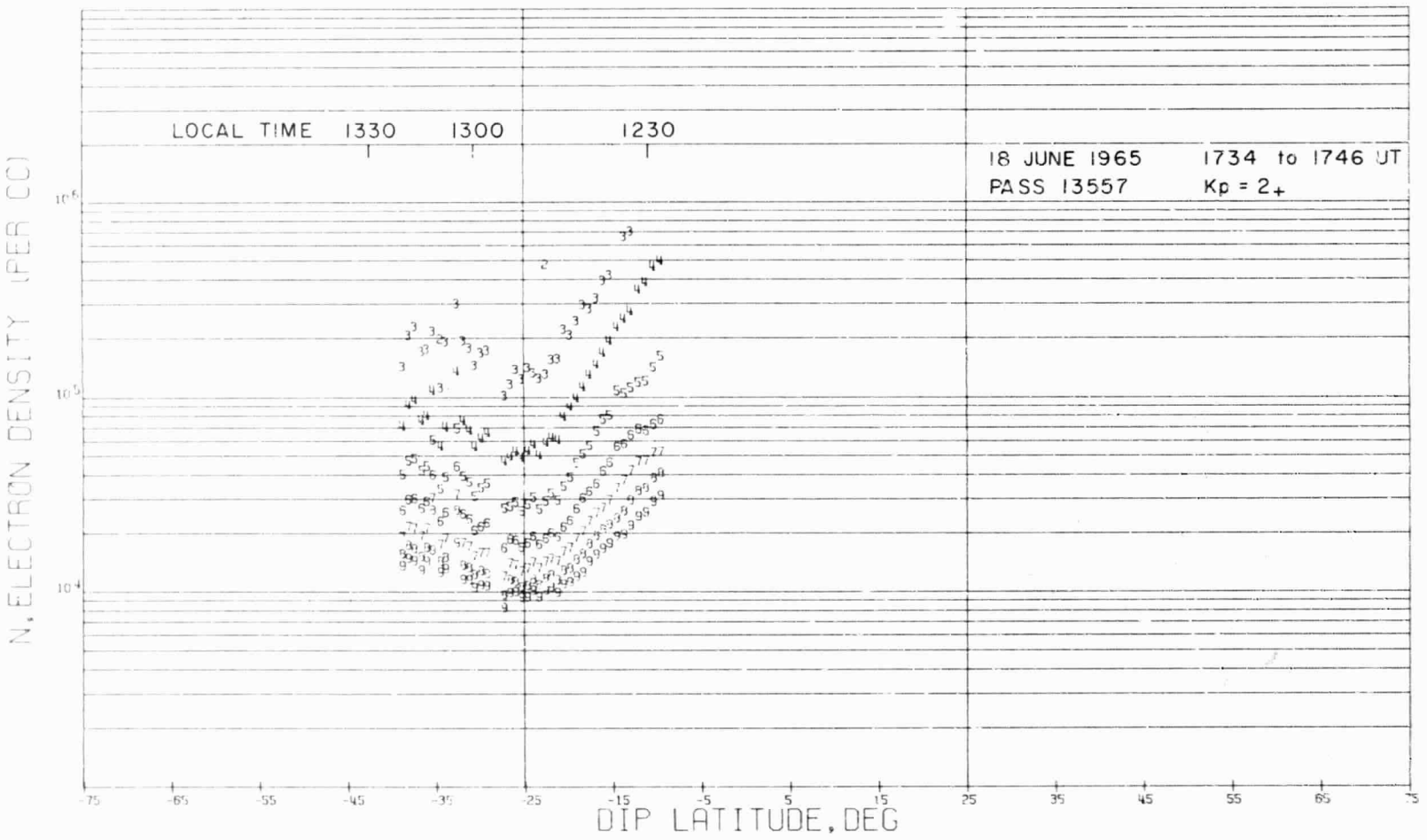

LATITUDINAL VARIATIONS OF N(e) ON JUNE 18, 1965

FIGURE 6.8

which re-establishes itself at the 400 km height level with peaks at magnetic latitudes of -8^{o} and $+15^{o}$. The equatorial maximum is noticeable at lower heights and displays a diminishing of ionization towards the higher latitudes. Referring to Figure 6.8, the N_e distribution on 18 June at low latitudes, a well-defined deep trough is seen to be situated near -25^{o} magnetic latitude, corresponding to a similar trough found in the latitudinal distributions of N_e on 16 and 17 June.

Constant altitude contours of N(e) for five satellite passes on 13, 15, 16, 17, and 18 June describing the behavior of the ionosphere in a comparative manner under both quiet and disturbed conditions, are presented in Figures 6.9 through 6.11 as a function of magnetic latitude. The median local time of the satellite passes for these five days was determined to be 1200 and the approximate universal time to be 1700 hours. The storm sudden commencement (SSC) began at roughly 1100 hours UT on 15 June, thus identifying the 15 June, 1246 to 1329 LMT, density contour as corresponding to the magnetic storm sudden commencement. Identifiable in Figures 6.10 through 6.11 is a moderate rise in N(e) on 15 and 16 June beyond that of 13 June, particularly at the lower latitudes, whereas there is a significant depression of N(e) on 17 June below that of the control day except for a peak near $+5^{o}$ at 400 km, with a gradual recovery towards the

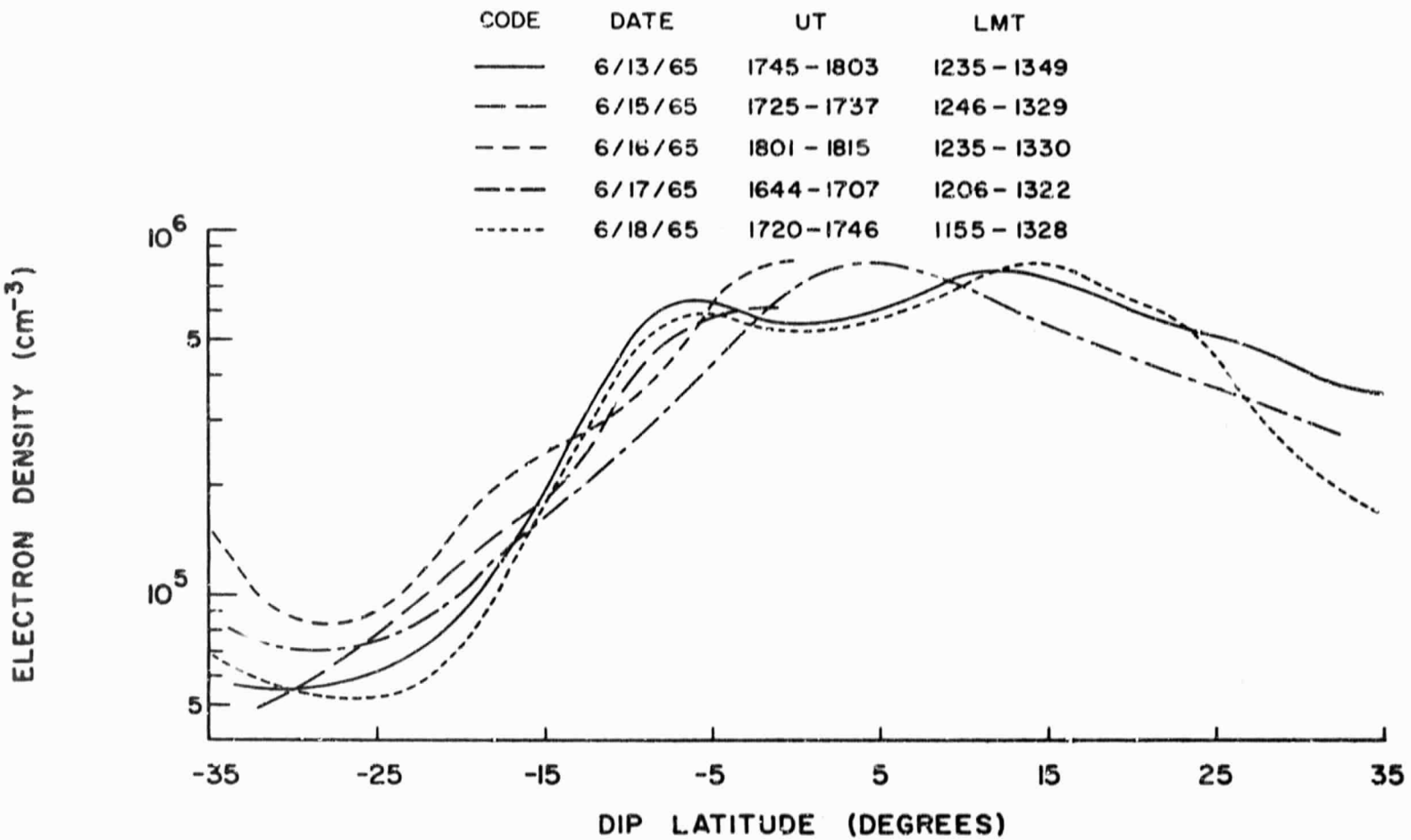

LATITUDINAL VARIATIONS OF N(e) AT 400 km DURING THE JUNE 15, 1965 MAGNETIC STORM

FIGURE 6.9

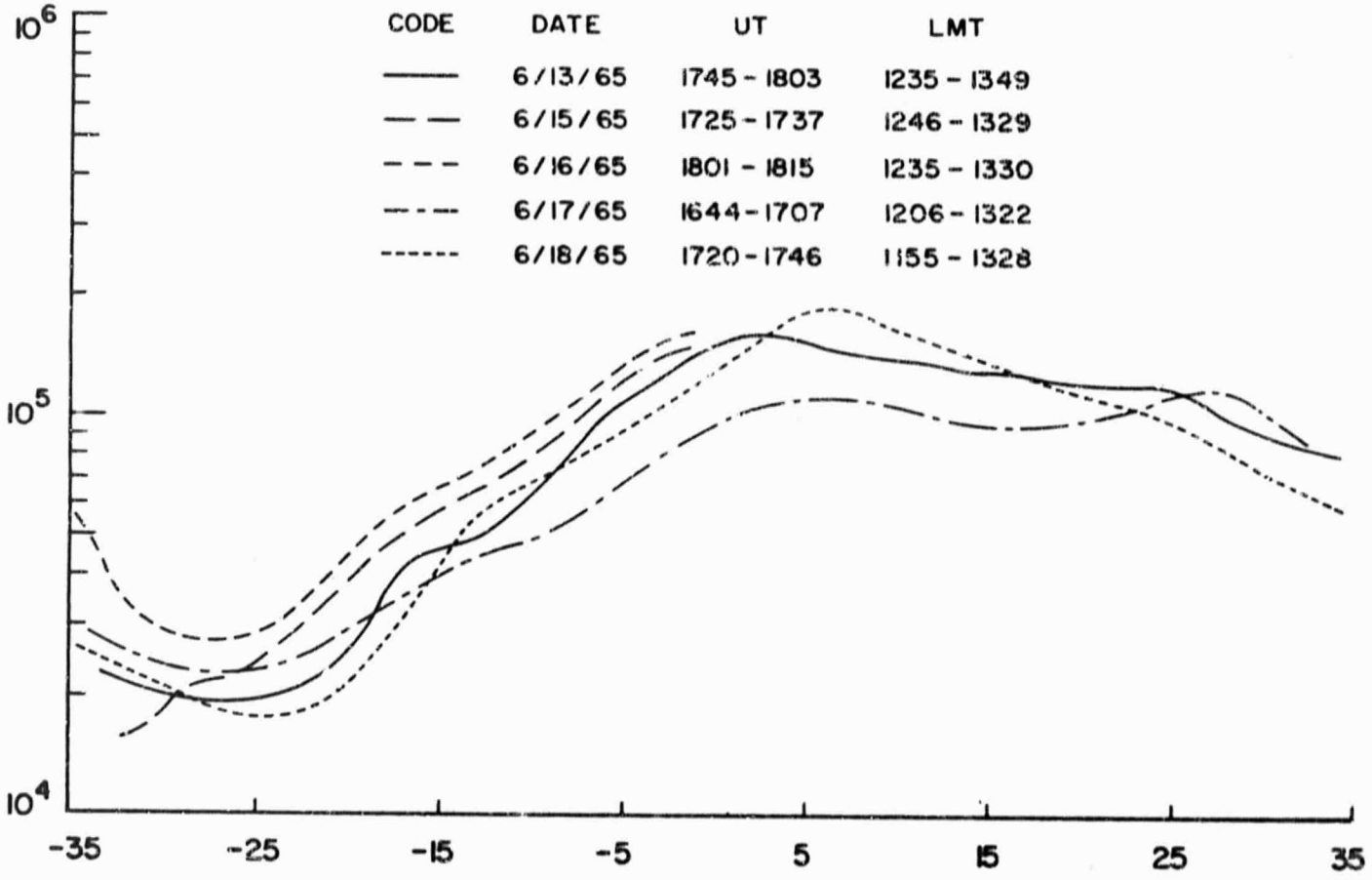

LATITUDINAL VARIATIONS OF N(e) AT 600 km
DURING THE JUNE 15, 1965 MAGNETIC STORM

FIGURE 6.10

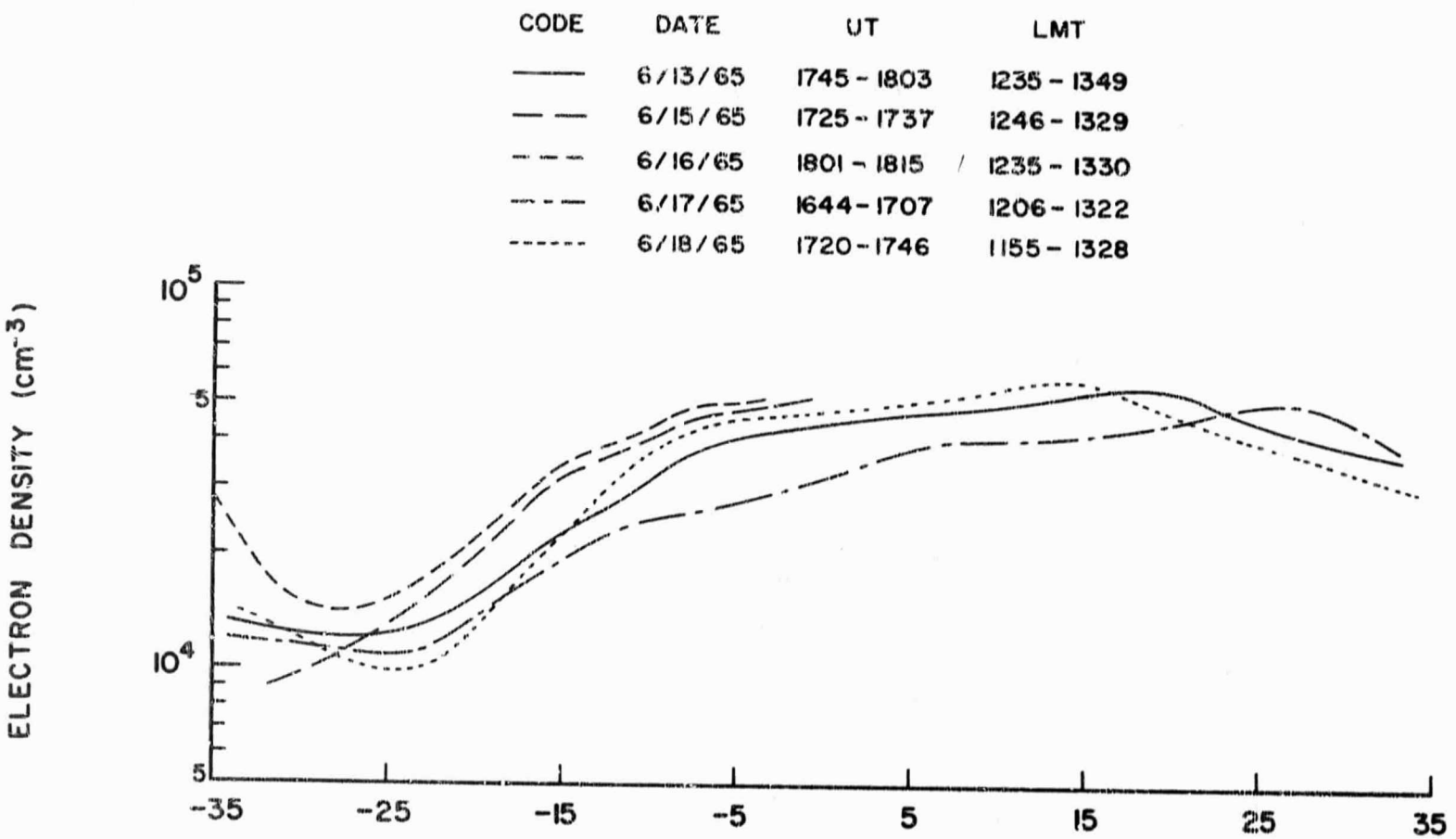

LATITUDINAL VARIATIONS OF N(e) AT 800 km DURING THE JUNE 15, 1965 MAGNETIC STORM

FIGURE 6.11

pre-storm quiet day ionization levels on 18 June, corresponding to the recovery phase of the magnetic storm. The behavior of N(e)(increasing) at 600 and 800 km on 15 and 16 June corresponds to the initial (positive) phase of the magnetic storm.

6.1.2 Plasma Scale Height Variations

Vertical scale heights of the vertical electron density distribution were computed at 100 km height increments between the F region peak and the height of the satellite. Latitudinal contours of Hv at the 400, 600, and 800 km height levels for the June 15 storm days are displayed in Figures 6.12 through 6.14.

Variations of Scale Height at 400 km: The latitudinal plot of Hv at 400 km on 13 June, the pre-storm quiet day, displays a peak centered near the magnetic equator; characteristic of quiet day behavior and correlated with the shape of the F2 peak. The F2 peak is thin in the mid-latitudes and thicker at the low and near-equatorial latitudes, producing a peak in the latitudinal plots of Hv near the magnetic equator. This peak is present up to 400 and 500 km, the magnitude decreasing with increasing altitude and disappearing beyond 600 km. The peak disappears on the disturbed day of 17 June and the contour on the disturbed day of 15 June, though limited in coverage, indicates that the peak is reduced. This may be interpreted as indicating that the F2 layer shape changes under disturbed conditions, becoming thinner as in the

mid-latitudes due to an increase in NmF2. From roughly 15^{o} to 35^{o} in the Northern hemisphere, the scale heights increase with latitude, forming a peak near 28^{o} magnetic latitude. However, in the Southern hemisphere, the scale heights are greater than the quiet day values from roughly 8^{o}S to 23^{o}S with a small maximum near 18^{o}S; Hv then decreases from 23^{o}S to 35^{o}S.

Variations of Scale Heights at 600 km: The 600 km vertical scale heights do not display any appreciable variation from $+35^{o}$ down to -10^{o}. Thereafter, from -10^{o} to -35^{o}, the disturbed day scale heights fall below the quiet day values of 13 June displaying a small but steady increase with latitude.

Variations of Scale Heights at 800 km: The quiet day scale heights on 13 June are more or less constant (Hv = 250 km) from 35^{o}N to 5^{o}N, where they begin increasing into the Southern hemisphere. Beyond -5^{o}, Hv increases rapidly reaching a maximum of 550 km near -25^{o}, decreasing thereafter with increasing latitude.

During the initial phase on 15 June, the peak seems to collapse, reappearing on 16 June but with a reduced magnitude. The disturbed day scale heights are lower than the quiet day values from -35^{o} to near -10^{o}, where they cross over with the disturbed day Hv possessing the higher values up to 12^{o}N. The maximum at 25^{o}S on 13 June is replaced by a minimum on the disturbed day 17 June. Thereafter, the same general trend of the 16 June

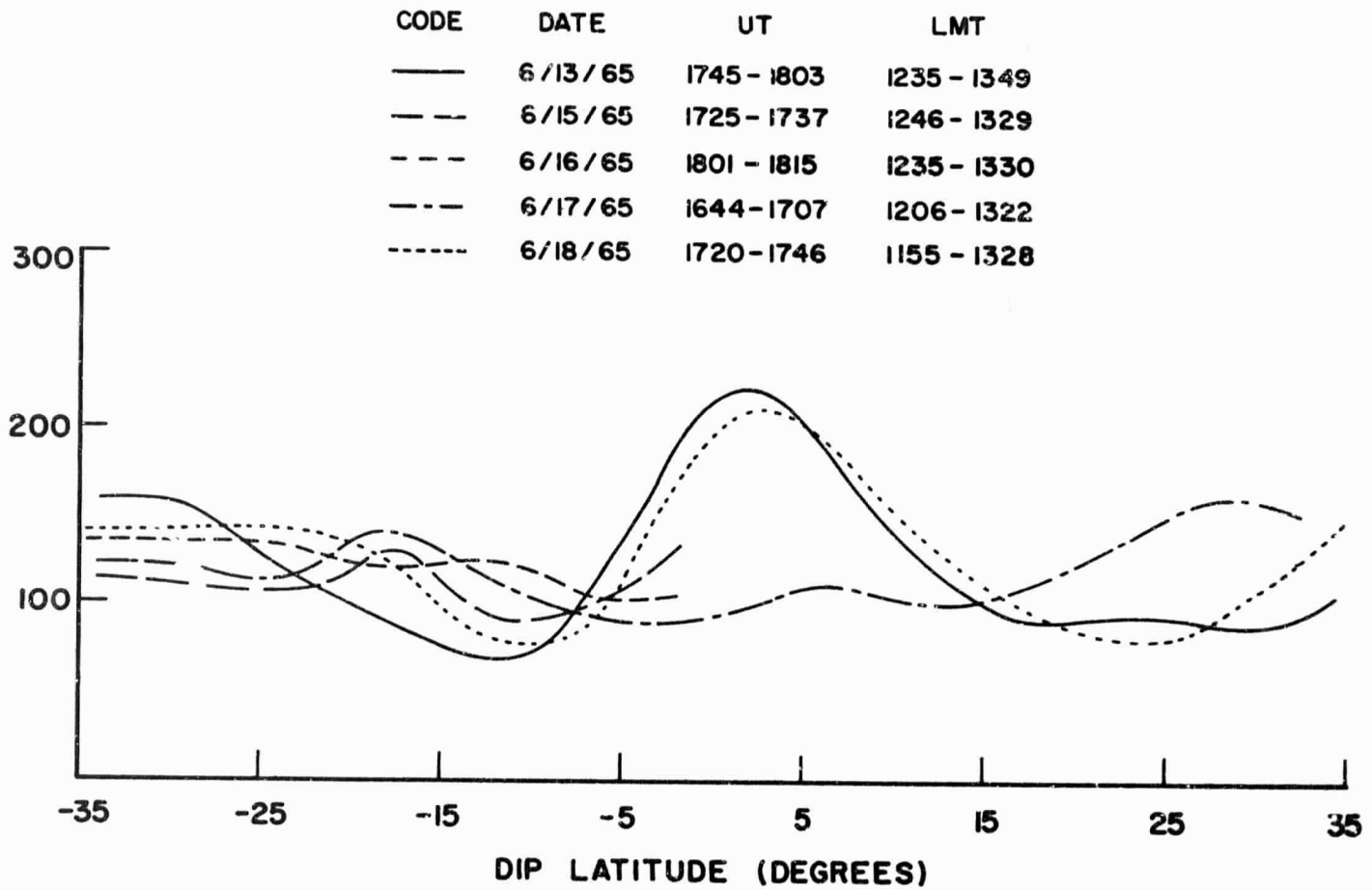

LATITUDINAL VARIATIONS OF Hv AT 400 km
DURING THE JUNE 15, 1965 MAGNETIC STORM

FIGURE 6.12

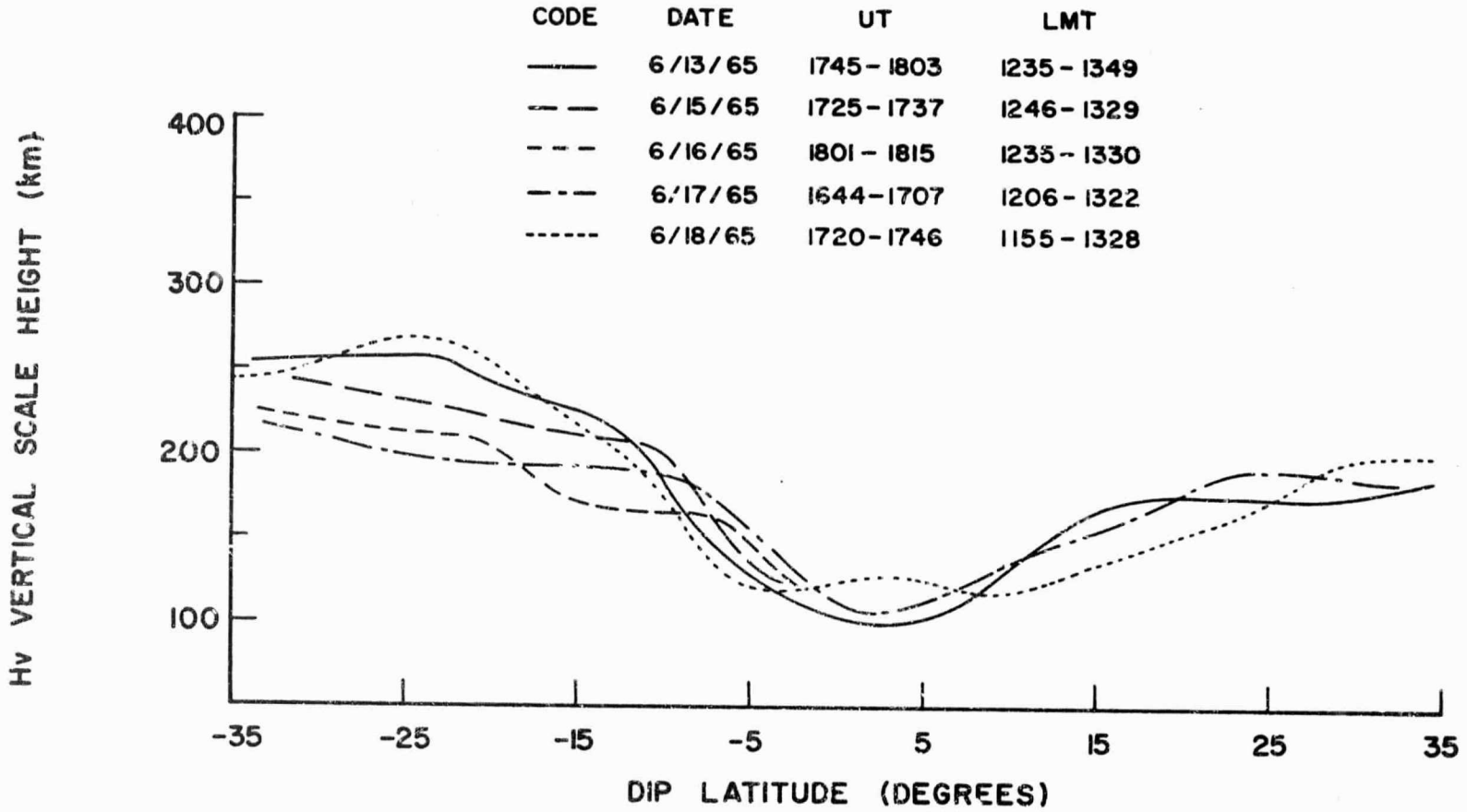

LATITUDINAL VARIATIONS OF Hv AT 600 km
DURING THE JUNE 15, 1965 MAGNETIC STORM

FIGURE 6.13

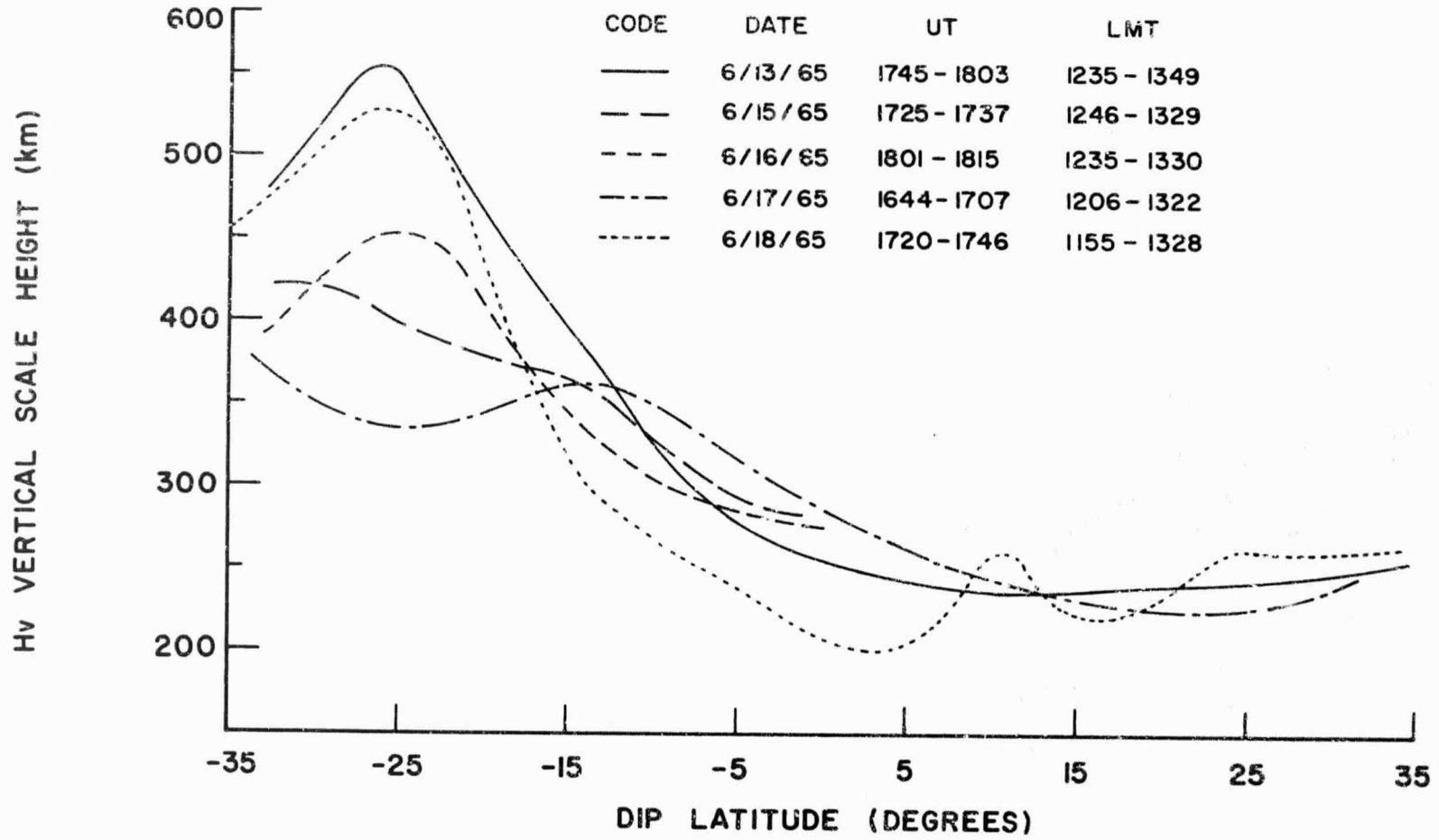

LATITUDINAL VARIATIONS OF Hv AT 800 km
DURING THE JUNE 15, 1965 MAGNETIC STORM

FIGURE 6.14

contours is followed; namely, higher scale height values in the near-equatorial region. From 14°N to 35°N, Hv is lower than on the quiet day. During the recovery phase on 18 June, the latitudinal contour tends to recover and follow the quiet day contour.

Rao (1968) finds for the June 15, 1965 storm at 30°N latitude, that Te on the disturbed day does not display any significant increase during the daytime, while Ti displays a decrease below 500 km. Thus, assuming that the plasma temperature at 800 km on the disturbed day is not considerably different from the quiet day value, large reductions in scale height in the 15°S to 35°S latitude range may be interpreted in terms of an increase in the mean ionic mass. The largest change takes place near 25°S by a factor of 1.67 on 17 June and 1.22 on 16 June. Titheridge and Andrews (1967), from measurements of the total electron content at Auckland, New Zealand (magnetic latitude of 21°S), infer an increase in the mean ionic mass by a factor of two. From Figure 6.14, for a similar dip latitude in the western hemisphere the mean ionic mass was found to increase by a factor of 1.41 on 17 June.

6.1.3 Variations of the Field Line Distribution of Electron Density

In order to gain a better insight into the physical processes responsible for the disappearance of the geomagnetic anomaly under magnetically disturbed conditions, graphs of the field line distribution of N(e) versus magnetic latitude and field line length were constructed.

Referring to Figure 6.15, significant depletions are immediately apparent at the upper regions, whereas farther down corresponding field lines, there is a significant build-up of ionization at the higher latitudes. This may be interpreted as a possible redistribution of N(e) within the magnetic tubes of force, probably caused by transport processes acting down the field lines. The intersection of corresponding field lines denotes the transition region and marks the magnetic latitudes (12^{o}N and 10^{o}S magnetic latitude) where ionization build-ups commence. Notice in particular that the lower field lines (those below 500 km) display a build-up of ionization near the magnetic equator, whereas the field lines above 500 km display depletions, strongly indicating the presence of vertical transport processes. Similar conclusions may be deduced from Figure 6.16 where variations of the field line distribution of N(e) versus s length (distance along the field lines) are presented. Here it may be seen that ionization depletions are displayed during the disturbed day at the upper field lines (those beyond 500 km) as compared to those of the quiet day 13 June; while significant ionization concentrations on corresponding field lines are realized at greater s lengths (higher latitudes). This again suggests a redistribution of ionization down the field lines by transport processes.

Maeda and Sato (1959) have shown that the quiet day drift velocity Vq, acts upward and northward in the

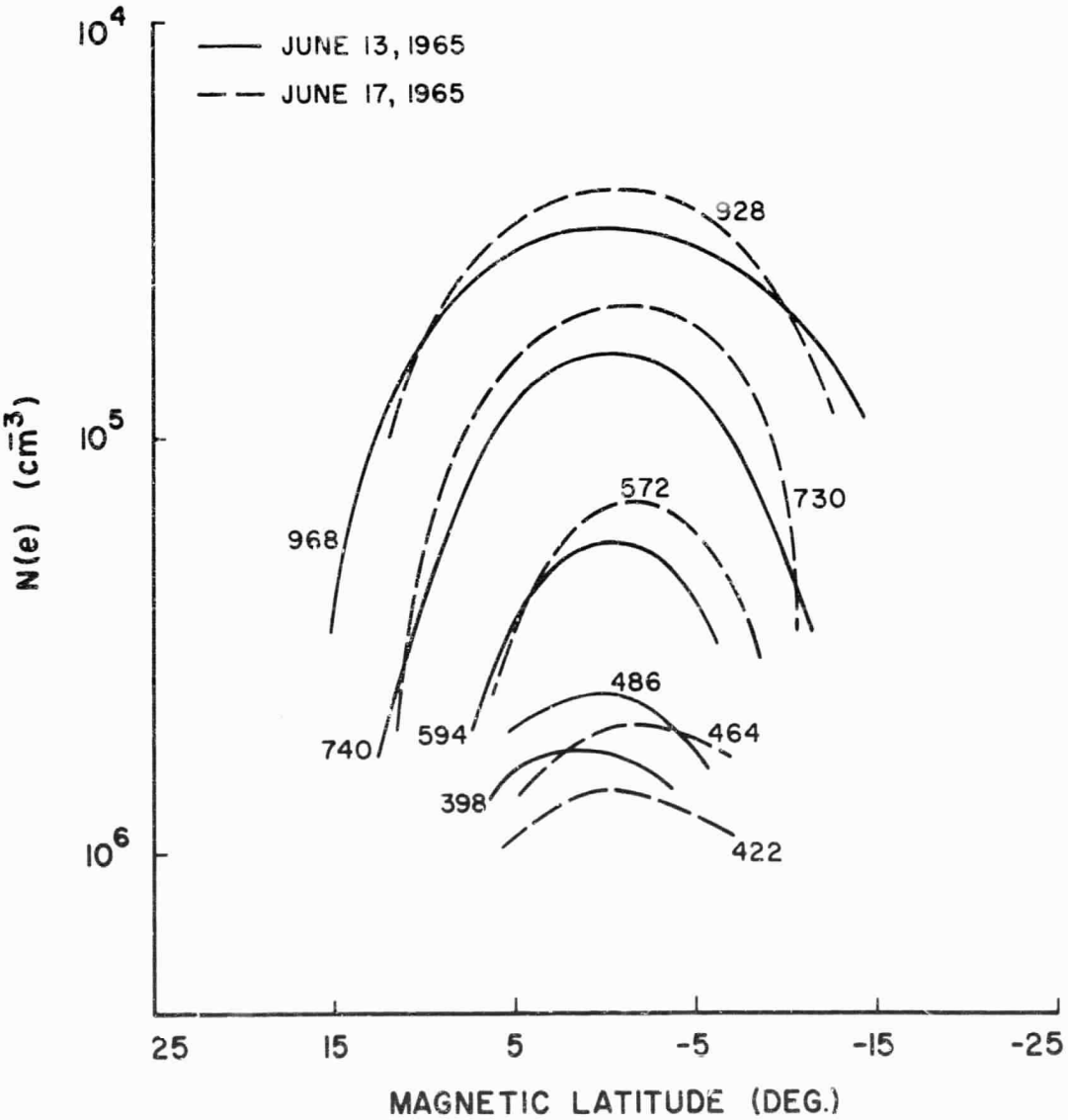

DISTRIBUTION OF N(e) ALONG MAGNETIC FIELD LINES

FIGURE 6.15

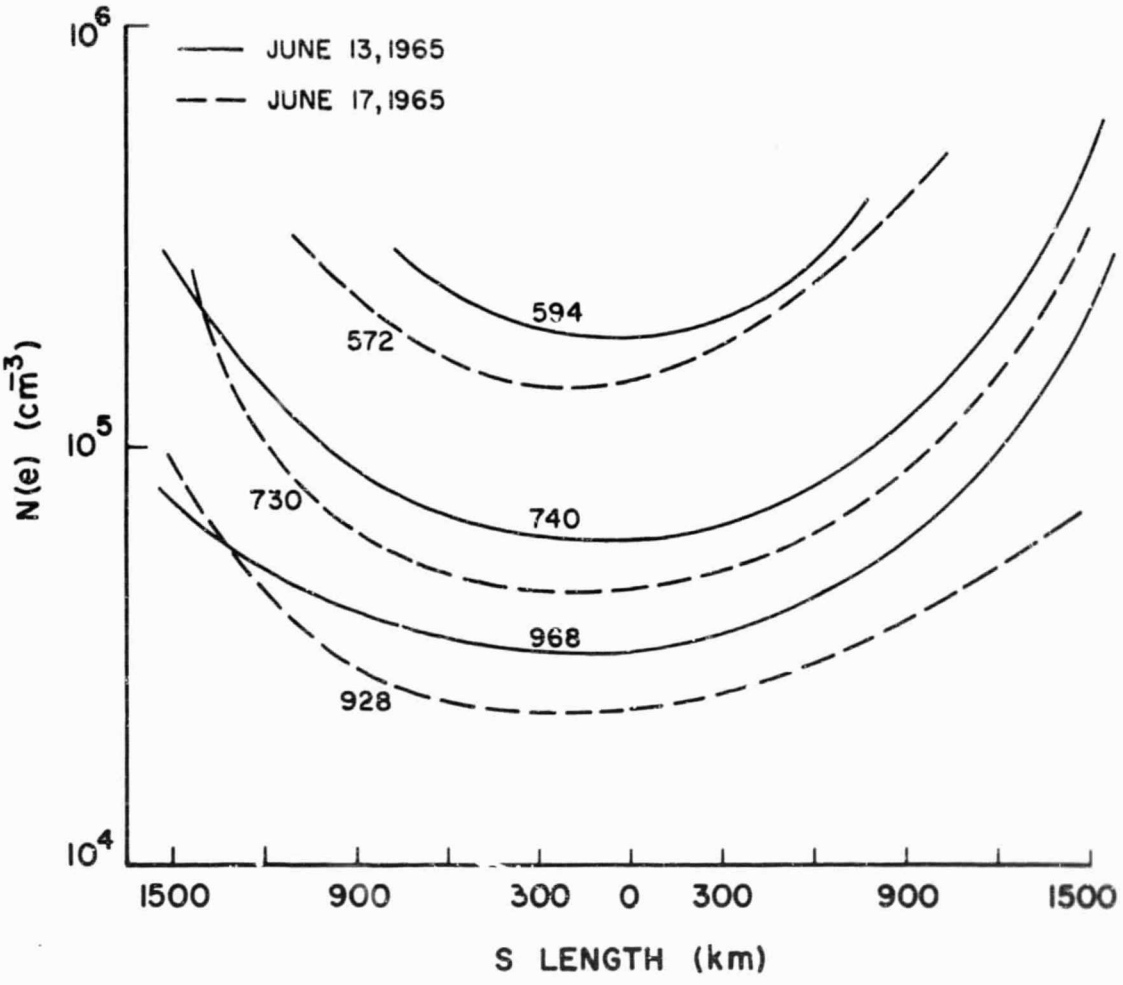

VARIATIONS OF N(e) WITH DISTANCE ALONG MAGNETIC FIELD LINES

FIGURE 6.16

northern hemisphere, being perpendicular to the geomagnetic field lines. Recently Sato (1968) interpreted the storm-time behavior of the anomaly in terms of vertical drift velocities (Hanson and Moffett, 1966). Sato proposes that if the disturbed day drift velocity Vd, which proceeds in the reverse direction to that of Vq at the near-equatorial latitudes, is comparable in magnitude to Vq, then the N(e) profile is the same as in the no-drift case on a quiet day. This implies that there is a vertical transport of N(e) under disturbed conditions so as to create an increase in N(e) concentrations in the lower topside ionosphere and corresponding N(e) depletions in the upper ionosphere. This is very much the same behavior as demonstrated by the field line distributions of N(e) in Figures 6.15 and 6.16.

6.2 March 8, 1963 Storm Analysis

Second of the magnetic storms to be investigated was the moderate storm commencing March 8, 1963 during which time the Kp index attained a maximum value of 6_o on 10 March. The pre-storm days of March 5-7, were decidedly quiet, while throughout the succeeding storm days of March 8-12, values of Kp remained inflated. March 7 was selected as the pre-storm quiet control day, the planetary magnetic index Kp never exceeding 2 in value on that day. Ionospheric data, pertaining to the magnetic storm of 8 March, analyzed and interpreted in the following discussion was derived from Electron Densities and Scale Heights in the Topside Ionosphere: Alouette I

Observations Over the American Continents - Volume II: March and May, 1963, by Chan, Colin, and Thomas (1966) and the corresponding graphical presentations of the latitudinal variations of electron densities and vertical scale heights (Figure 6.17 through Figure 6.22 were derived from Electron Densities and Scale Heights in the Topside Ionosphere: Alouette I Observations Over the American Continents - Volume IV: Summary Graphs, by Chan, Colin, and Thomas (1967).

6.2.1 Electron Density Variations

Constant altitude contours of N(e) for the storm days of 8, 9, 10, and 11 March during the 8 March magnetic storm describing the behavior of the disturbed ionosphere, with 7 March included as the pre-storm control day, are presented in Figures 6.17 through 6.19 as a function of magnetic latitude. The mean local time of the satellite passes during these storm days was determined to be roughly 1330.

There is a moderate rise of ionization at 400 km and a moderate depression of ionization at 600 and 800 km on 8 March ($Kp = 4_+$), the first day of the storm, near the magnetic equator. Particularly significant on this day is the disappearance of the anomaly at 400 km though it was present on 7 March ($Kp = 2_+$) the pre-storm quiet control day, with a single ionization maximum subsequently replacing it at the magnetic equator. There is a decided increase in ionization on 9 March ($Kp = 3_-$) at all height

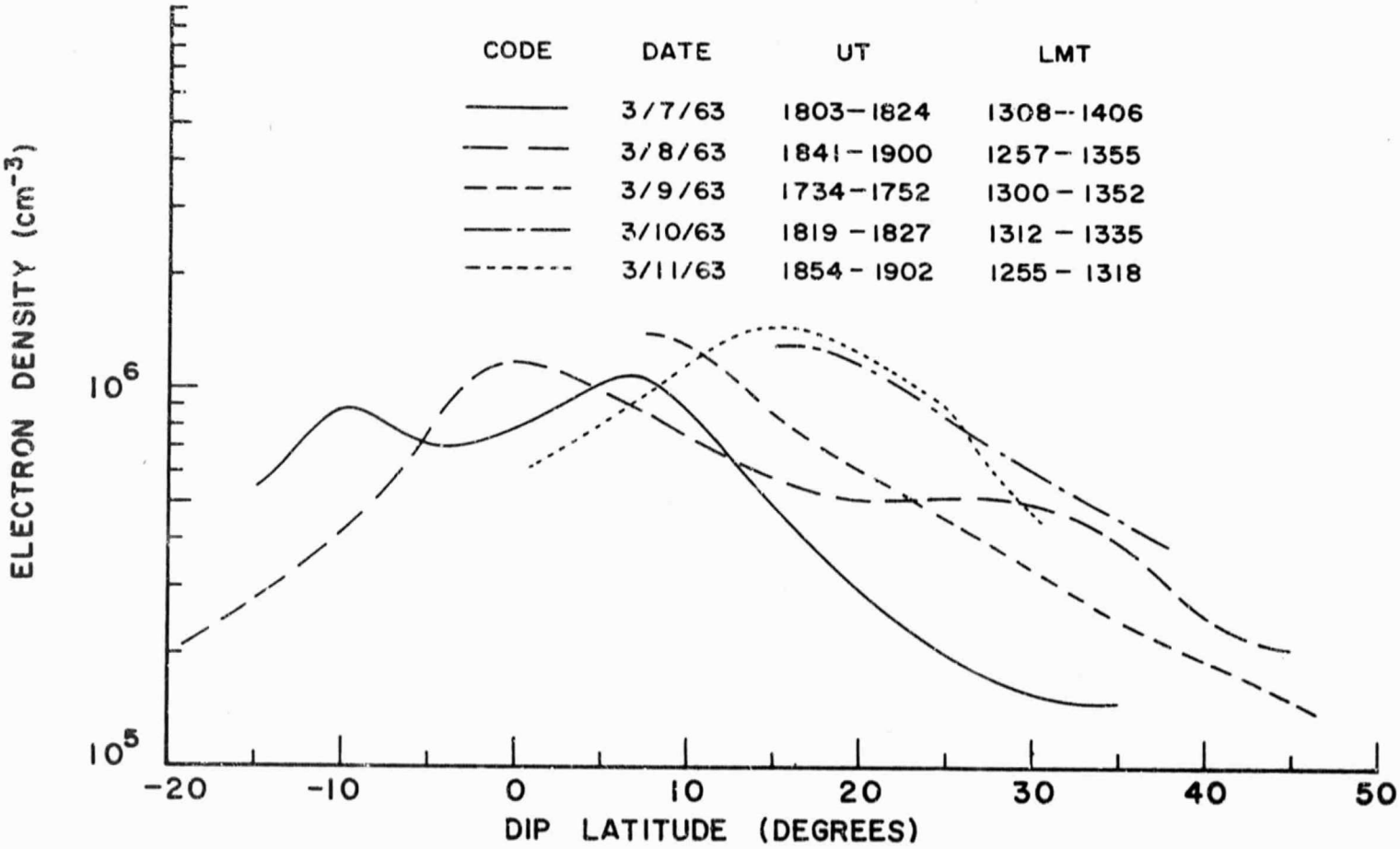

LATITUDINAL VARIATIONS OF N(e) AT 400 km DURING THE MARCH 8, 1963 MAGNETIC STORM

FIGURE 6.17

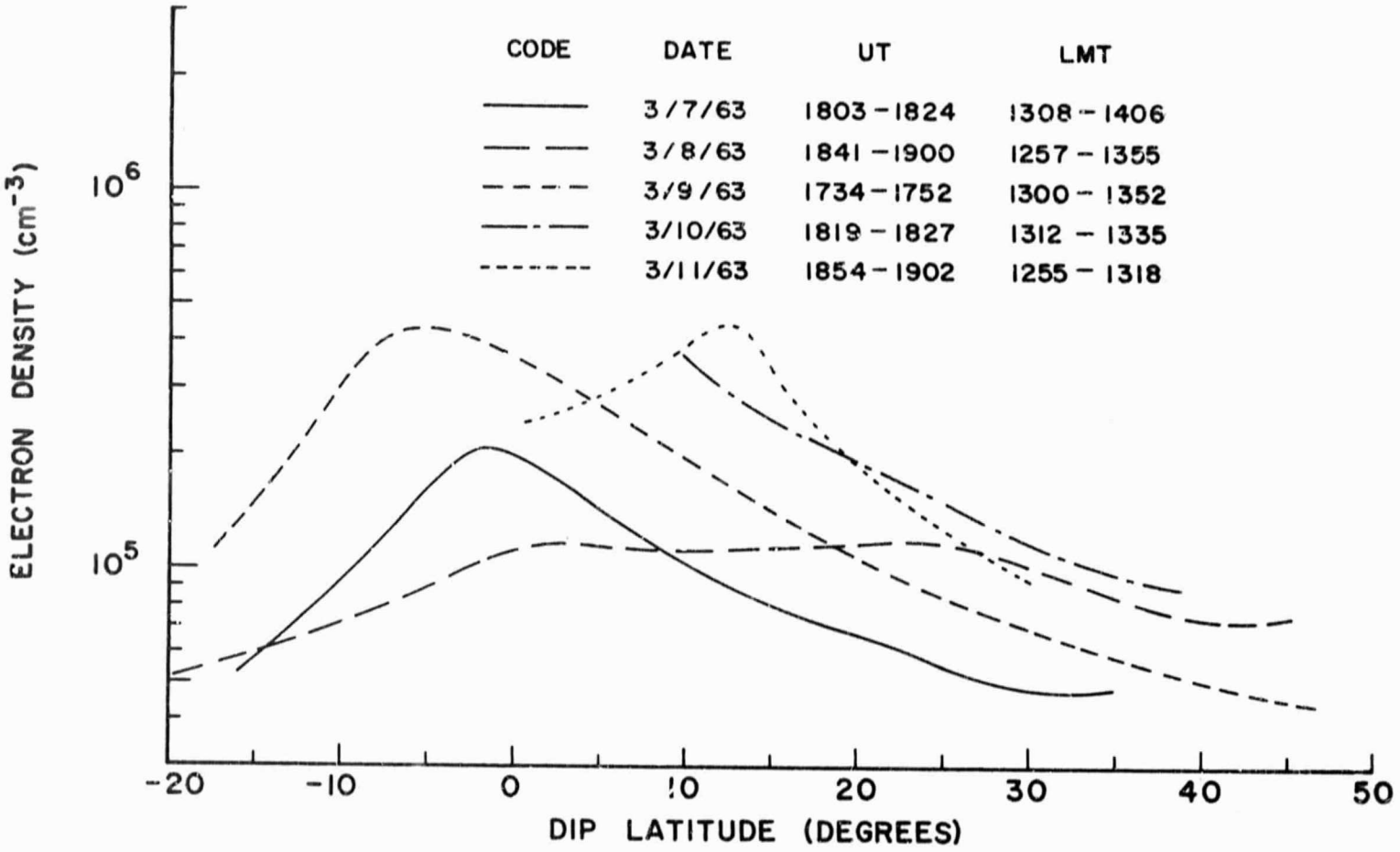

LATITUDINAL VARIATIONS OF N(e) AT 600 km
DURING THE MARCH 8, 1963 MAGNETIC STORM

FIGURE 6.18

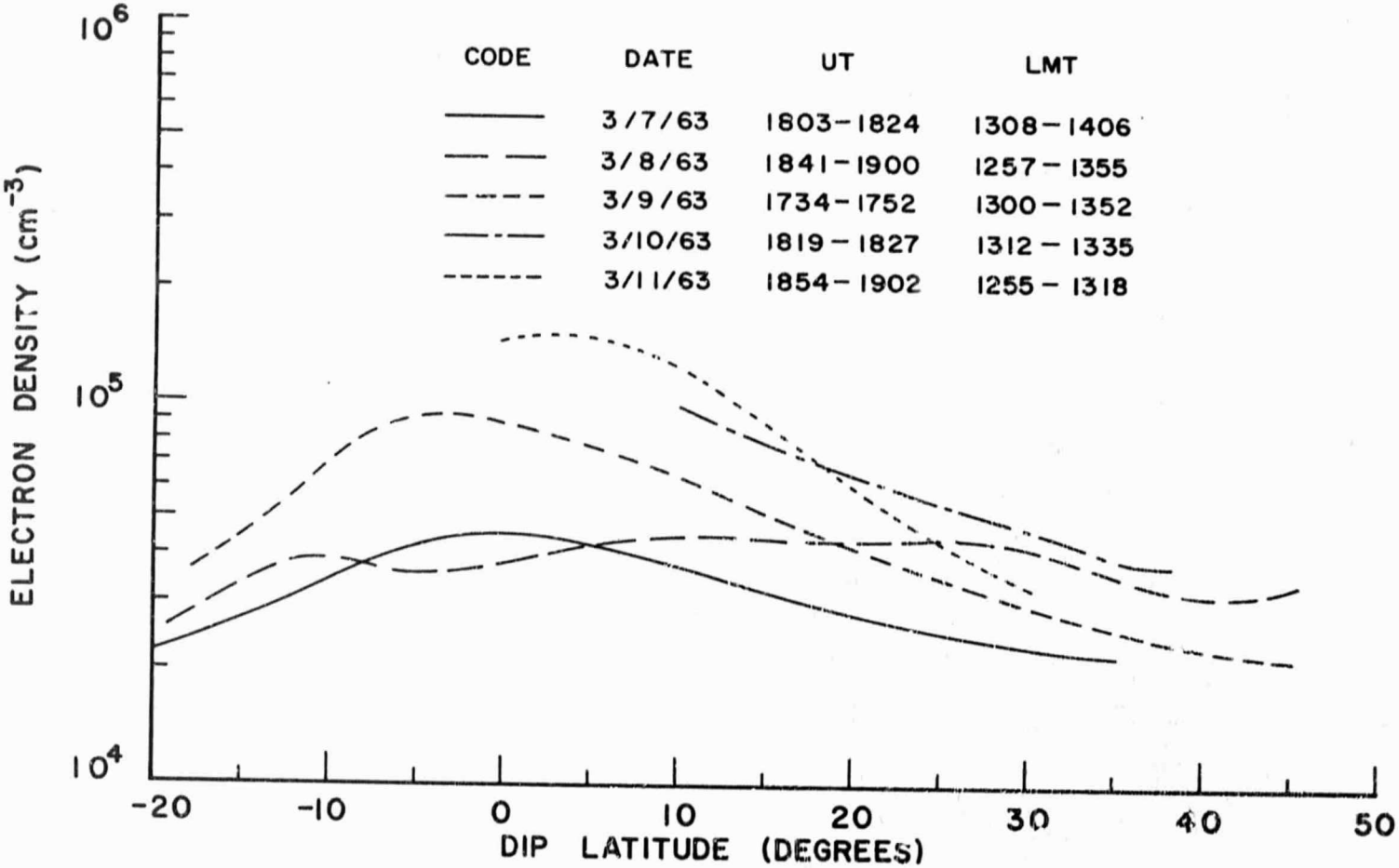

LATITUDINAL VARIATIONS OF N(e) AT 800 km
DURING THE MARCH 8, 1965 MAGNETIC STORM

FIGURE 6.19

levels compared to that of the control day, the increase being smaller at greater height levels. This decided increase in N(e) on 9 March persists and intensifies on 10 March ($Kp = 6_o$) and sustains itself on 11 March at all height levels. The crests of ionization reappearing on 11 March ($Kp = 4_+$) at 400 and 600 km near 15^oN magnetic latitude, is a positive indication of the impending return of the anomaly. Positive identification is lacking though due to limited latitudinal coverage. There is no apparent indication of the anomaly at 800 km prior or subsequent to the magnetic storm.

The asymmetrical character of the June storm N(e) distribution about the magnetic equator as compared to the March storm N(e) distribution, may be interpreted as being attributable to seasonal effects. Thus, the behavior of the anomaly during the March storm, which was significantly similar to that during the June storm, substantiates the June storm findings and corroborates the conclusion that when $Kp > 6$ during the storm main phase, the anomaly completely disappears.

6 2.2 Plasma Scale Height Variations

Latitudinal contours of the vertical scale heights at the 400, 600, and 800 km height levels for the March 8 storm days are displayed in Figures 6.20 through 6.22.

Variations of Scale Height at 400 km: The latitudinal plot of Hv at 400 km on 7 March, the pre-storm quiet day displays a peak near the magnetic equator. This is also characteristic of quiet day behavior, corresponding to a similar peak found in the Hv contour at 400 km on 13 June. The peak disappears on 8 March corresponding to a similar disappearance of the Hv peak on the disturbed day of 17 June, depicting significantly reduced scale heights below those of the control day near the magnetic equator (-15^{o} to $+ 10^{o}$ magnetic latitude). There is also noticeable in Figure 6.20 a significant depression of the disturbed day values of Hv at magnetic latitudes of 25^{o}N and higher. The Hv contour of 11 March tends to recover toward the quiet day contour of 7 March.

Variations of Scale Height at 600 km: Referring to Figure 6.21, most significant in the Hv contour at 600 km is the continued depression of disturbed day scale heights below these of 7 March at magnetic latitudes of 10^{o}N and higher.

Variations of Scale Heights at 800 km: From an analysis of Figure 6.22, there is apparent a marked increase in Hv on 8 March near the magnetic equator compared to the quiet control day, which displays a significant depression there, increasing into the southern hemisphere and remaining rather constant from roughly 10^{o}N to 38^{o}N. There follows, on 9 March, a pronounced depression in Hv at the magnetic equator, corresponding to a similar depression in Hv

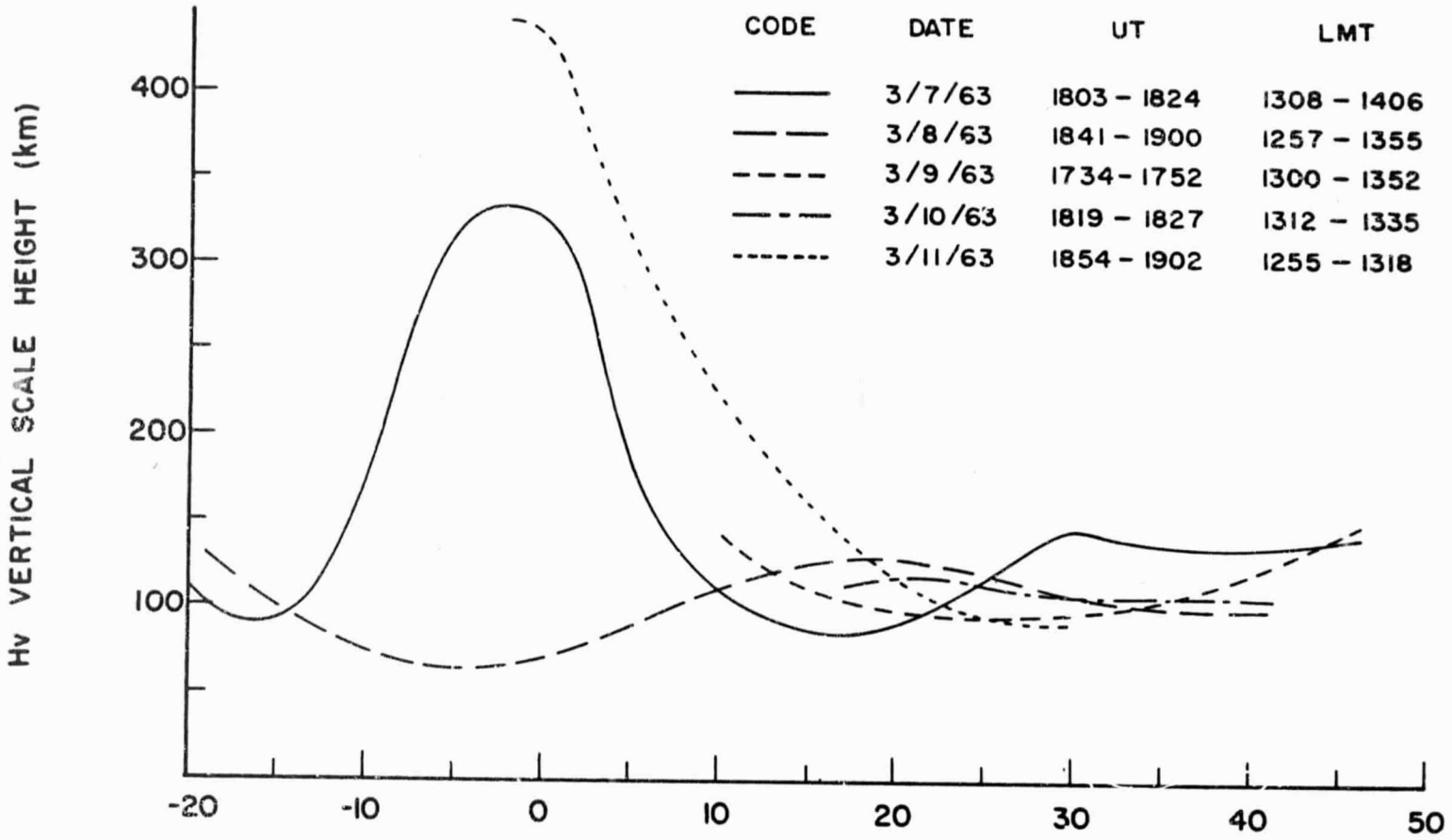

LATITUDINAL VARIATIONS OF Hv AT 400 km
DURING THE MARCH 8, 1963 MAGNETIC STORM

FIGURE 6.20

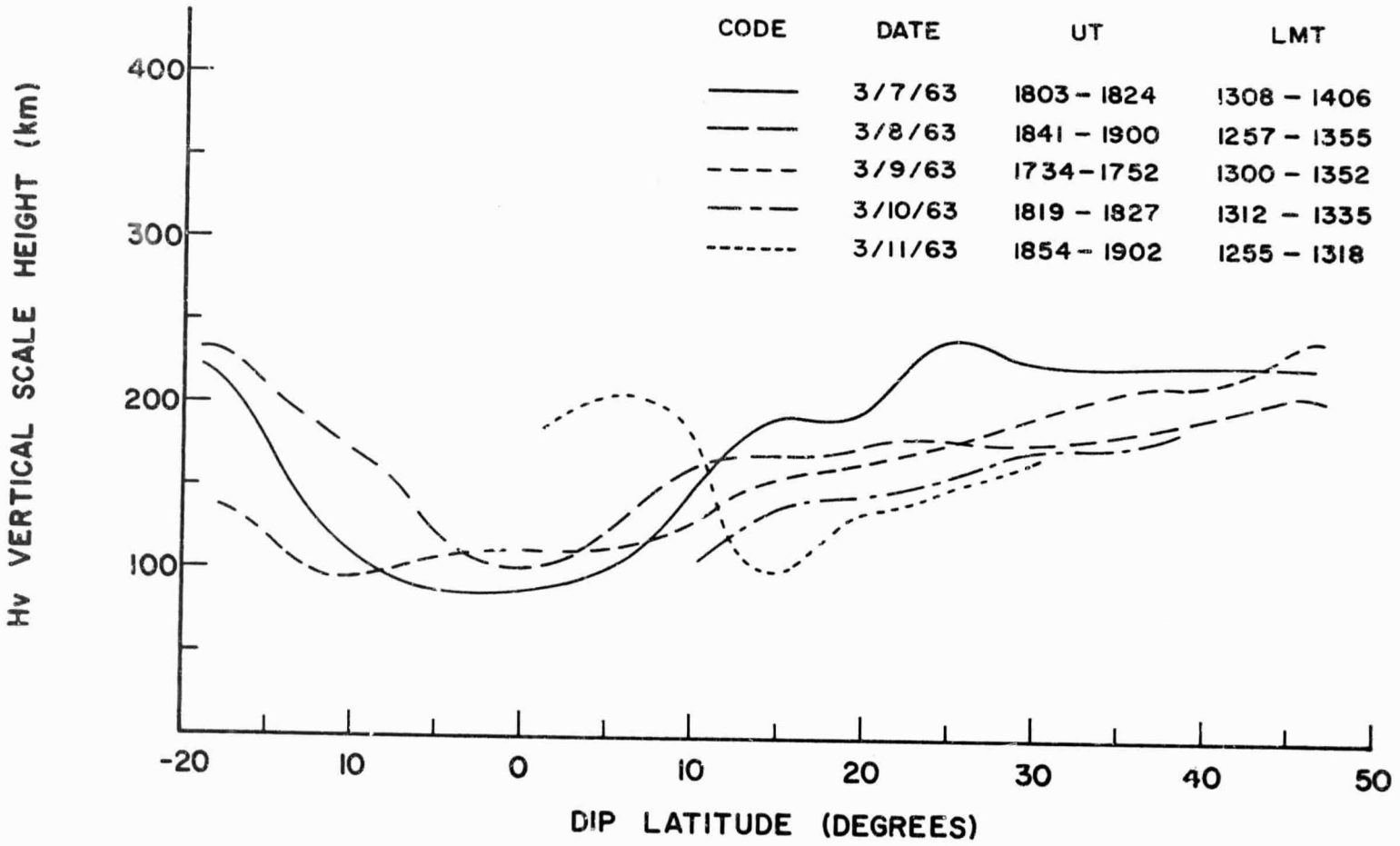

LATITUDINAL VARIATIONS OF Hv AT 600 km
DURING THE MARCH 8, 1963 MAGNETIC STORM

FIGURE 6.21

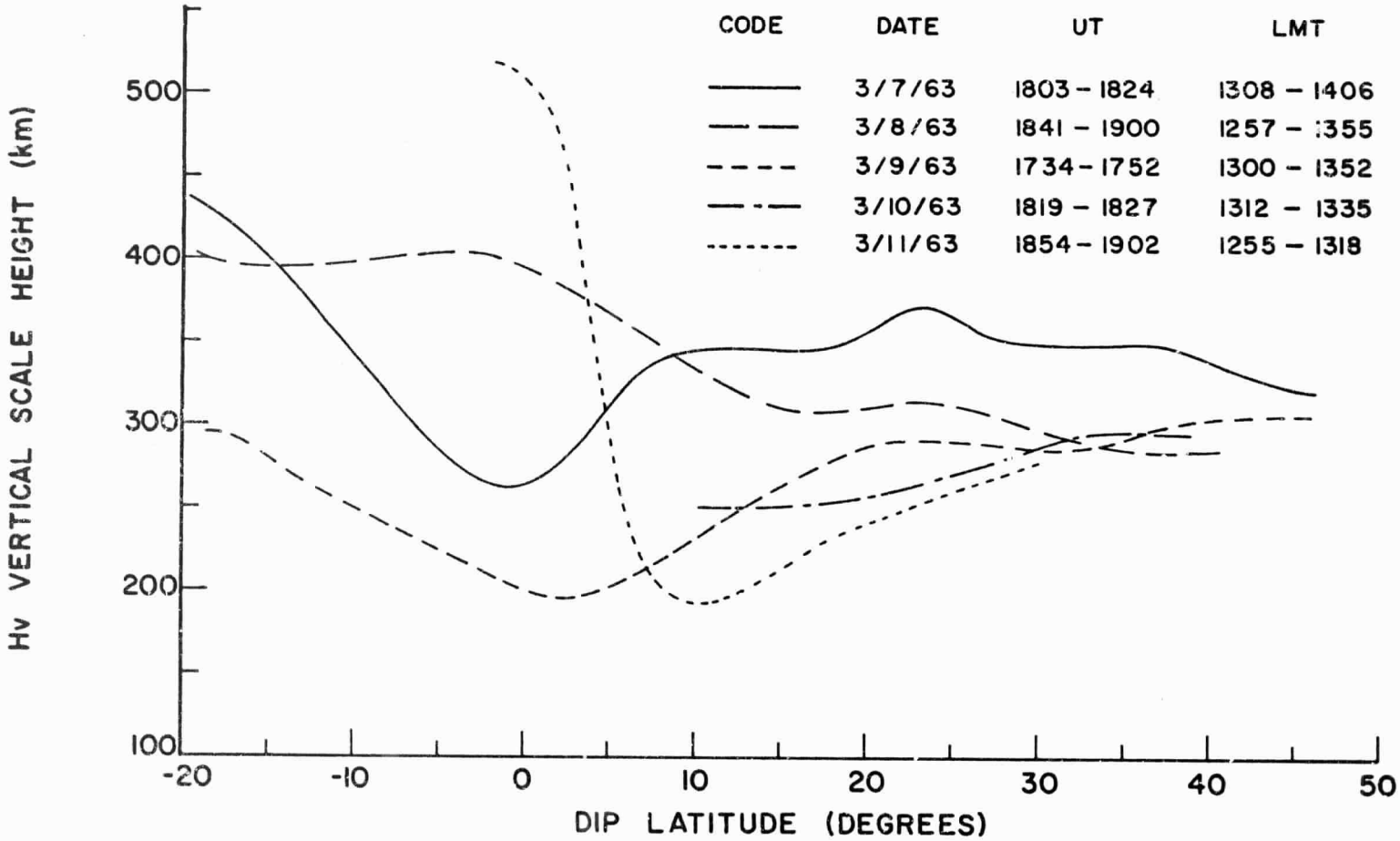

LATITUDINAL VARIATIONS OF Hv AT 800 km
DURING THE MARCH 8, 1963 MAGNETIC STORM

FIGURE 6.22

exhibited during the June storm main phase. Furthermore, disturbed day values of Hv are found to fall significantly below those of the quiet day values from 10^{o}N magnetic latitude and higher on 8, 9, 10, and 11 March. This implies as in the June storm, increased values of mean ionic mass (under the continuing assumption of insignificant temperature changes).

CHAPTER VII

SUMMARY AND CONCLUSIONS

From a detailed investigation of two magnetic storms, significant and consistent features of the storm behavior of the topside ionosphere are derived. Particular attention was devoted to the June 15, 1965 magnetic storm; specifically, the collapse of the anomaly and subsequent interpretation of this collapse in terms of ionization transport processes. Furthermore, substantiation of the collapse of the anomaly under high magnetic activity was gained from the analysis of the March 8, 1963 storm. The interpretation of these changes is presented in the present chapter with the intention of identifying, if possible, the physical mechanisms responsible for the topside ionosphere storm behavior.

Lyon and Thomas (1963) suggested that the diurnal behavior of the anomaly was correlated with fluctuations in magnetic activity, while Lockwood and Nelms (1964) related the commencement of the anomaly with magnetic activity. More recently, King et al. (1967) indicated that the trough of the anomaly becomes shallower under weak ($Kp \leq 4$) disturbances. Basu and Das Gupta (1968) and Sato (1968) have most recently reported similar conclusions and suggest the correlation between Kp and the geomagnetic anomaly is rather vague. However, the results presented here demonstrate that whenever during a

moderately severe magnetic storm Kp exceeds a value of roughly 6, the geomagnetic anomaly disappears. The work of previous authors seems to show that the depth of the anomaly near-equatorial trough is decreased with increasing Kp. Therefore, we suggest that there is a distinct correlation between Kp and the behavior of the geomagnetic anomaly, which vanishes only during moderately severe magnetic storms (Kp > 6).

Variations in N(e) of the topside ionosphere in response to the June magnetic storm was represented by moderate enhancements on 15 and 16 June, corresponding to the magnetic storm positive initial phase. Ionization enhancements, corresponding to the storm main phase, were identified on 16 June and 9 and 10 March storm days.

Furthermore, a decided depression of N(e) on 18 June identifies the ionosphere recovery phase, which lags behind the magnetic storm recovery phase. Thus, these results illustrate the dependence of the storm-time N(e) variations upon the phase of the magnetic storm.

Substantial and consistent reduced values of the vertical scale height Hv were detected throughout all of the magnetic storms investigated. These reduced values of Hv persist in spite of recognized increases in the neutral temperature during magnetic storms (Jacchia and Slowey, 1964) which would imply higher storm-time values of Hv. This then strongly suggests the postulation of an increased mixing of the ionosphere, raising the normal diffusive

separation height level resulting in an increase in the mean ionic mass, thereby driving down the disturbed day scale height values (Titheridge and Andrews, 1967 and Bauer and Krishnamurthy, 1967).

BIBLIOGRAPHY

1. Alfven, H., Tellus, 1, 50, 1955.

2. Allen, C. W., Terr. Mag. Atm. Electr., 53, 507, 1948.

3. Appleton, E. V., and Barnett, N. F., Nature, 115, 333, 1925.

4. Appleton, E. V., and Ingram, G. D. C., Nature, 136, 548-549, 1935.

5. Appleton, E. V., and Piggott, W. R., J. Atm. Terr. Phys., 2, 236, 1952.

6. Basu, S., and Gupta, A. D., JGR, 73, 5599, 1968.

7. Bauer, S., Report X-615-65-155, GSFC, 1965.

8. Bauer, S., and Jackson, J. E., JGR, 67, 1703, 1962.

9. Bauer, S. J., and Krishnamurthy, B. V., Report X-615-67-576, GSFC, 1967.

10. Berkner, L. V., Seaton, S. L., and Wells, H. W., Terr. Mag. and Atm. Elec., 44, 283, 1939.

11. Chandra, S., and Goldberg, R. A., JGR, 69. 3187, 1964.

12. Chapman, S., Proc. Phys. Soc. 43, 1931.

13. Chapman, S., Terr. Mag. Atmos. Elec., 40, 349, 1935.

14. Chapman, S., Vistas in Astronomy, Pergammon Press, Vol. II, 1956.

15. Chapman, S., and Bartels, T., Geomagnetism, Oxford Press, Vol. I, 1940.

16. Chapman, S., and Ferraro, V. C., Terr. Mag. Atmos. Elec., 36, 77, 1931; 37, 147, 1932; 38, 79, 1933.

17. Cole, K. D., JGR, 69, 3595, 1964.

18. Doupnik, J. R., and Schmerling, E. R., Report 230, Ionosphere Research Laboratory, The Pennsylvania State University, 1965.

19. Dressler, A. J., Hanson, W. B., and Parker, E. N., JGR, 66, 3631, 1961.

20. Dressler, A. J., and Parker, E. N., JGR, 64, 2239, 1959.

21. Evans, J. V., JGR, 70, 2726, 1965.

22. Fukushima, N., and Hayasi, T., Rep. Ionos. Res. Japan, 5, 85, 1952.

23. Garriott, O. K., and Rishbeth, H., Plan. Sp. Sci., 11, 587, 1963.

24. Groves, G. V., Rep. Univ. College, London, 1961.

25. Hanson, W. B., and Moffett, R. J., JGR, 71, 5559, 1966.

26. Hibbard, F. H., and Ross, W. J., JGR, 72, 5331, 1967.

27. Hinteregger, H. E., and Watanbe, K., JGR, 67, 1810, 1962.

28. Hirono, N., Rep. Ionos. Res. Japan 9, 95, 1955.

29. Jacchia, L. G., Sp. Res. II, 747, 1961.

30. Jackson, J. E., Report X-615-67-452, GSFC, 1967.

31. Kamiyama, H., Sci. Rep. Tohoku Univ., 7, 125, 1956.

32. King, J. W., Reed, K. C., Olatunji, E. O., and Legg, A. J., J. Atm. Terr. Phys. 29, 1355, 1967.

33. King, J. W., Smith, P. A., Ecclas, D., Fooks, G. F., and Helm, H., Proc. Roy. Soc., 281, 464, 1964.

34. Knecht, R. W., JGR, 64, 1243, 1959.

35. Lockweed, G. E., and Nelms, G. L., J. Atm. Terr. Phys., 26, 569, 1964.

36. Lyon, A. J., and Thomas, L. J., Atm. Terr. Phys., 25, 373, 1963.

37. Maeda, K., Rep. Ionos. Res. Japan, 7, 81, 1953.

38. Maeda, K., Rep. Ionos. Res. Japan 9, 71, 1955.

39. Maeda, K., and Sato, T., Proc. Inst. Radio Eng., 47, 232, 1959.

40. Martyn, D. F., Nature, 167, 92, 1951.

41. Martyn, D. F., Proc. Roy. Soc., 218, 1, 1958.

42. Martyn, D. F., Phys. of Ionosphere, 1955.

43. Matsushita, S., JGR, 5, 109, 1953.

44. Matsushita, S., JGR. 54, 309, 1959.

45. Matsushita, S., JGR, 68, 2595, 1963.

46. Matsuura, N., J. Rad. Res. Lab. Japan, 10, 1, 1963.

47. Meek, J. H., JGR, 58, 445, 1953.

48. Nagata, T., and Oguti, T., Rep. Ionos. Res. Japan, 7, 21, 1953.

49. Nisbet, J. S., and Quinn, T. P., JGR, 68, 1517, 1963.

50. Obayashi, T., Rep. Ionos. Res. Japan, 6, 69, 1952.

51. Obayashi, T., Rep. Ionos. Res. Japan, 8, 135, 1954.

52. Obayashi, T., Research in Geophysics, M.I.T. Press, 325, 1964.

53. Odishaw, H., Research in Geophysics, M.I.T. Press, 1964.

54. Ondoh, T., J. Rad. Res. Lab., 76 267, 1967.

55. Piddington, J. H., JGR, 65, 93, 1960.

56. Quinn, T. P., and Nisbet, J. S. JGR, 70, 1205, 1965.

57. Rao, P. B., JGR, 73, 1661, 1968.

58. Reddy, B. M., Bruce, L. H., and Findlay, J. A., JGR, 72, 2709, 1967.

59. Rishbeth, H., Plan. Sp. Sci., 11, 31, 1963.

60. Rishbeth, H., Proc. IEEE, 55, 16, 1967.

61. Rishbeth, H., and Barron, D. W., J. Atm. Terr. Phys., 18, 234, 1960.

62. Rishbeth, H., and Setty, C., J. Atm. Terr. Phys., 20, 263, 1964.

63. Rishbeth, H., Van Zandt, T. E., and Morton, R. B., ESSA, 1966.

64. Sato, T., J. Geomag. Geoelect., 8, 129, 1956; 9, 94, 1957.

65. Sato, T., JGR, 73, 6225, 1968.

66. Sayers, J., Proc. Rey. Soc. London, 281, 450, 1964.

67. Seaton, N. J., J. Atm. Terr. Phys., 8, 122, 1956.

68. Singer, S. F., Trans. Am. Geophys. Union, 38, 175, 1957.

69. Sinno, K., Rep. Ionos. Res. Japan 7, 7, 1953; and 8, 127, 1954.

70. Sinno, K., Rep. Ionos. Res. Japan, 9, 166, 1955.

71. Somayajulu, Y. V., JGR, 65, 893, 1960.

72. Somayajuly, Y. V., JGR, 68, 1899, 1963.

73. Stubbe, P., J. Atm. Terr. Phys., 30, 243, 1968.

74. Thomas, L., JGR, 71, 1357, 1966.

75. Thomas, J. O., Briggs, B. R. Colin, L., Rycroft, M. J., and Covert, M., NASA TN D-2882, 1965.

76. Thomas, J. O., and Robbins, A., J. Atm. Terr. Phys., 1958.

77. Thomas, J. O., Rycroft, J. M. Colin, L., and Chon, K. L., Proc. NATO Adv. Study Inst., 1965.

78. Thomas, L., and Venebles, F. H., J. Atm. Terr. Phys., 28, 599, 1966.

79. Titheridge, J. E., and Andrews, M. K., Plan Sp. Sci., 15, 1157, 1967.

80. Wilmore, A. P., and Handerson, C. L., Space Res., 5, 241, 1965.

81. Yonezawa, T., Proc. Int. Conf. Ionos., 128, 1963.

82. Yonezawa, T., Sp. Sci Rev., 5, 1204, 1966.